



Response of Drainage Pattern and Basin Evolution to Tectonic and Climatic Changes Along the Dinarides-Hellenides Orogen

L. Gemignani^{1*}, B. V. Mittelbach^{1,2}, D. Simon¹, A. Rohrmann¹, M. U. Grund¹, A. Bernhardt¹, K. Hippe¹, J. Giese^{1,3} and M. R. Handy¹

¹Institut für Geologische Wissenschaften, Freie Universität Berlin, Berlin, Germany, ²Geological Institute, Swiss Federal Institute of Technology (ETH) Zürich, Zürich, Switzerland, ³The Geological Survey of Norway (NGU), Trondheim, Norway

OPEN ACCESS

Edited by:

Gang Rao,
Southwest Petroleum University,
China

Reviewed by:

Huiping Zhang,
Institute of Geology, China Earthquake
Administration, China
Xianyan Wang,
Nanjing University, China

*Correspondence:

L. Gemignani
lorenzo.gemignani@fu-berlin.de

Specialty section:

This article was submitted to
Structural Geology and Tectonics,
a section of the journal
Frontiers in Earth Science

Received: 24 November 2021

Accepted: 10 March 2022

Published: 19 April 2022

Citation:

Gemignani L, Mittelbach BV, Simon D,
Rohrmann A, Grund MU, Bernhardt A,
Hippe K, Giese J and Handy MR (2022)
Response of Drainage Pattern and
Basin Evolution to Tectonic and
Climatic Changes Along the Dinarides-
Hellenides Orogen.
Front. Earth Sci. 10:821707.
doi: 10.3389/feart.2022.821707

The junction of the Dinaric and Hellenic mountain belts hosts a trans-orogenic normal fault system (Shkoder-Peja Normal Fault, SPNF) that has accommodated oroclinal bending, as well as focused basin formation and drainage of the Drin River catchment. Analysis of fluvial morphology of this catchment reveals higher values of river slope indices (k_{sn}) and χ (Chi) between the normal faults of the SPNF and the Drin drainage divide. The drainage divide is predicted to be migrating away from the SPNF, except at the NE end of the SPNF system. Two basins analysed in the hangingwall of the SPNF, the Western Kosovo Basin (WKB) and Tropoja Basin (TB), contain late Pliocene-to-Holocene sedimentary rocks deposited well after the main fault activity and immediately after the Last Glacial Maximum (LGM). These layers document an early Pleistocene transition from lacustrine to fluvial conditions that reflects a sudden change from internal to external drainage of paleo-lakes. In the TB, these layers were incised to form three generations of river terraces, interpreted to reflect episodic downstream incision during re-organisation of the paleo-Drin River drainage system. ³⁶Cl-cosmogenic-nuclide depth-profile ages of the two youngest terraces (~12, ~8 ka) correlate with periods of wetter climate and increased sediment transport in post-LGM time. The incision rate (~12 mm/yr) is significantly greater than reported in central and southern Albania. Thus, glacial/interglacial climatic variability, hinterland erosion and base-level changes appear to have regulated basin filling and excavation cycles when the rivers draining the WKB and TB became part of the river network emptying into the Adriatic Sea. These dramatic morphological changes occurred long after normal faulting and clockwise rotation on the SPNF initiated in late Oligocene-Miocene time. Faulting provided a structural and erosional template upon which climate-induced erosion in Holocene time effected reorganisation of the regional drainage pattern, including the formation and partial demise of lakes and basins. The arc of the main drainage divide around the SPNF deviates from the general coincidence of this divide with the NW-SE trend of the Dinaric-Hellenic mountain chain. This arc encompasses the morphological imprint left by roll-back subduction of the Adriatic slab beneath the northwestern Hellenides.

Keywords: drainage basin analysis, tectonic and climate interactions, central mediterranean, geomorphic metrics, cosmogenic ³⁶Cl exposure dating

INTRODUCTION

Drainage networks in orogens are sensitive to tectonics and climatic conditions (Lavé and Avouac, 2001; Whittaker et al., 2007; Whipple, 2009; Wobus et al., 2010; Kirby and Whipple 2012; Whittaker, 2012; Schwanghart and Scherler, 2020). These factors affect landscape morphology on the scale of continents, but the time scales on which they operate overlap on the scale of orogens, faults, and individual basins (Whipple and Tucker, 1999). The challenge here is to distinguish spatial and temporal controls on the landscape in an active orogen with a prolonged history of oroclinal bending. We investigate the junction of the Dinaric-Hellenic mountain belt on the Balkan Peninsula, where the retreating Adriatic slab has affected lithospheric deformation from Paleocene to Holocene time (e.g., Burchfiel et al., 2008; Handy et al., 2019). We use the Neogene intramontane drainage basins of Northern Albania and Kosovo to examine the competing effects of both past and present faulting, as well as transient Pliocene-Holocene climate on fluvial dynamics and landscape evolution.

Intramontane basins are either internally or externally drained depending on whether the river system draining the basin is connected with a lower base level (e.g., the sea). Thus, a change in the base level of a river in response to tectonic and/or climatic events can lead to the integration of river branches and landscape change (D'Agostino et al., 2001; Garcia-Castellanos, 2006; Harkins et al., 2007; Attal et al., 2008; Geurts et al., 2018; 2020). On the other hand, numerical models have shown that river capture and integration can themselves affect the local base level, producing pervasive changes in the river network geometry. Such transformations involve drainage divide migration and knickpoint mobility (e.g., Willett et al., 2014; Yang et al., 2015; Whipple et al., 2017). Several cycles of progressive basin filling and subsequent excavation characterize the spatio-temporal evolution of drainage basins. The basin gains or loses connectivity with the orogenic foreland (e.g., Aterno River in the Italian Apennines; see D'Agostino et al., 2001; Geurts et al., 2018). In either case, the fluvial system exerts a first-order control on the position and magnitude of sedimentary supply within the basin (Whittaker et al., 2007) which can be used to infer patterns of hinterland erosion (Braun et al., 2018; Gemignani et al., 2018).

The tectonics of the Dinaric-Hellenic mountain belt along the eastern shore of the Adriatic Sea (Figure 1A) accommodated Late Cenozoic shortening related to northwestward advance of the Adriatic Plate relative to Eurasia, and the southwestward retreat of the subducting Adriatic slab beneath the Hellenides (e.g., Jolivet and Brun, 2010; black arrows in Figure 1B). Slab rollback induced distributed extension of the upper plate of this subduction (Royden, 1996) which has affected crustal structure, landscape and drainage patterns from the Southern Balkans to the Aegean and Adriatic regions since the Late Paleocene to Present (e.g., Burchfiel et al., 2008). The rate of rollback subduction has increased to ~10 mm/yr since the Late Miocene (Jolivet and Brun, 2010).

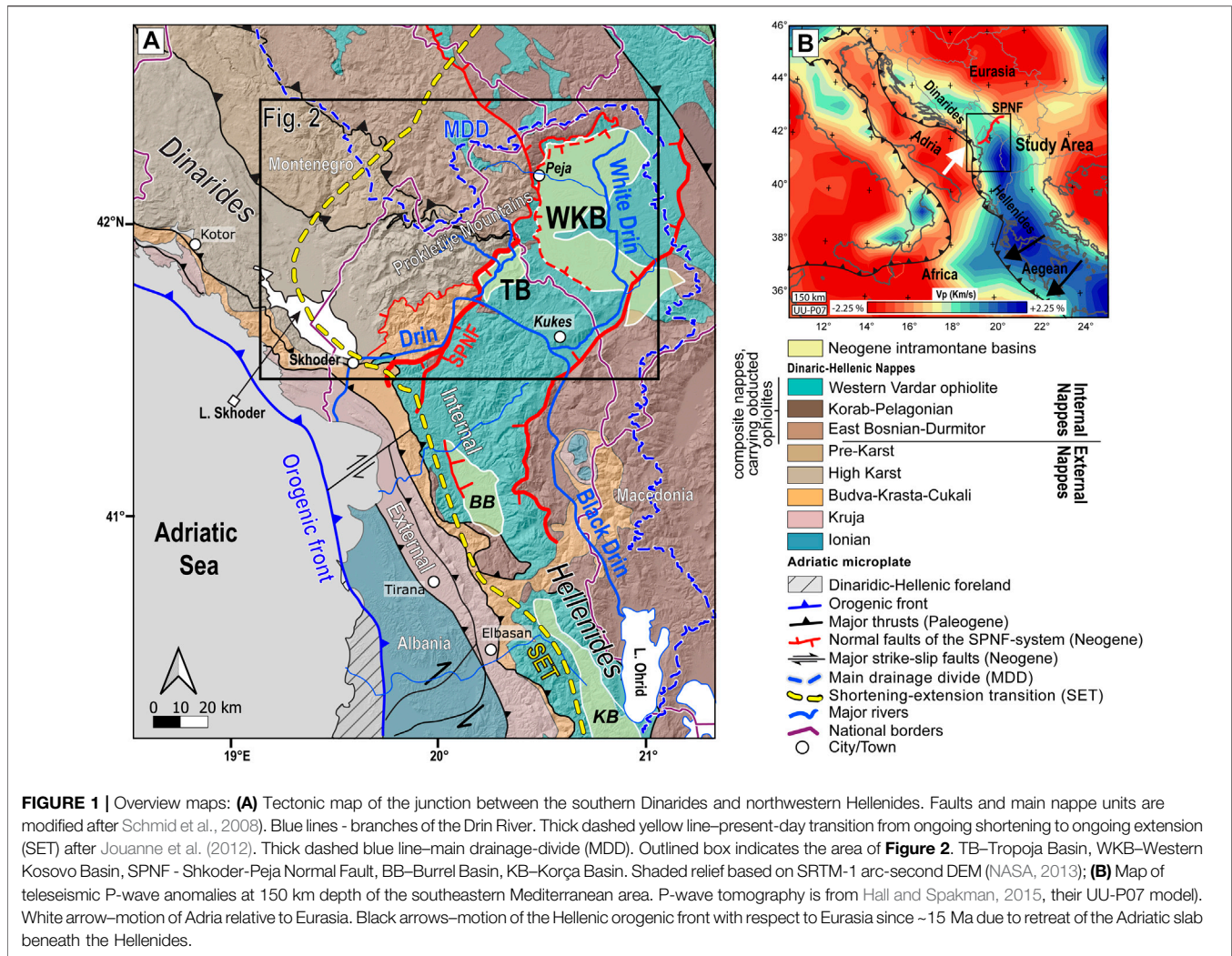
The junction of the Dinaric and Hellenic belts is an excellent place to study the competing effects of tectonics and climate on the fluvial network. This junction is the site of an oroclinal bend of some 20° (Figure 1) that coincides with an orogen-parallel transition in mantle structure from a detached shallow segment of the Adriatic slab beneath the Dinarides to a long attached segment of the same slab to the south beneath the Hellenides (high Vp domains in blue in Figure 1B, Wortel and Spakman 2000; Piromallo and Morelli 2003; Handy et al., 2019). This junction coincides with a system of faults, most prominent among them the Shkoder-Peja Normal Fault (SPNF, Figure 1A), that cut across the orogen (Burchfiel et al., 2008; Schmid et al., 2008; Handy et al., 2019). Paleomagnetic studies indicate that bending started in Paleogene time, but increased markedly in Neogene time (Kissel et al., 1995; Speranza et al., 1995; Muceku et al., 2008). The bend in the orogen coincides with Cenozoic intramontane basins and an anomalous drainage pattern, including arcuation of the main drainage divide (MDD, dashed blue line in Figure 1) around the orogen (Figure 1).

The Drin River at the Dinaric-Hellenic junction in northern Albania (Figure 1) originates at Ohrid Lake where it is called the Black Drin (Figure 1A), then runs to the NW for ~150 km parallel to the strike of the orogen before joining its northern branch, the White Drin, near the town of Kukes (Figure 1A). From there, the river cuts down to the SW through the West Vardar Ophiolite in a graben between conjugate normal faults of the SPNF system (thick red lines in Figure 1A). The Drin empties into the Adriatic Sea near the city of Shkoder (Figure 1A).

The present-day boundary between active orogenic shortening and extension defined in geodetic studies (Jouanne et al., 2012; D'Agostino et al., 2020) is referred to here as the shortening-extension transition (SET), signified by a dashed yellow line in Figure 1A. The SET trends across the nappe boundaries and also runs discordantly to the main drainage divide (blue dashed line in Figure 1A). The drainage divide is deflected to the NE around the SPNF and its related faults.

Two basins in the hanging wall of the SPNF, the Western Kosovo Basin and Tropoja Basin, contain middle Miocene-Pliocene and Plio-Pleistocene clastic and freshwater sediments, respectively (Figure 1A; Meço and Aliaj, 2000). These basins are interpreted to have formed during clockwise rotation of the Hellenic part of the orogen with respect to the Dinaric segment (Handy et al., 2019). We note that some Neogene normal faults and basins also strike parallel to the orogen (e.g., basins labelled BB and KB in Figure 1A) and form asymmetric half-grabens in the hanging wall of former Dinaric thrusts (Dumurdzanov et al., 2005; Burchfiel et al., 2008; Handy et al., 2019). The Neogene age of the graben fill coincides with thermochronometric ages of cooling and exhumation in the footwalls of the graben from ~23 Ma until to ~4 Ma (Muceku et al., 2008).

In this paper, we investigate tectonic and climatic processes affecting the evolution of river drainage at the Dinaric-Hellenic junction. Following an introduction to the geology and morphology of the basins and their catchments at this



junction, we provide descriptions of the stratigraphy and river terraces carved into the Tropoja Basin. This is followed by an outline of the methods used to characterize and date the landscape on scales ranging from this basin to the entire orogenic bend. A description of the basin stratigraphy and its river terraces is followed by a presentation of new ^{36}Cl exposure ages of these terraces. A morphometric analysis of the regional drainage network at the orogenic junction then lays the foundation for a discussion of how the river channel network has responded to tectonic uplift, erosion and climate since Pliocene time. We conclude with a conceptual model for the Pliocene-to-Present evolution of basins at the Dinaric-Hellenic junction. It is found that the Neogene fault system that accommodated oroclinal bending and Hellenic slab rollback is the main factor controlling morphology on the orogenic scale. Faulting and footwall uplift increased rocks' erodibility through fracturing and hill-slope degradation, whereas terrace incision and drainage integration through river capture events after the Last Glacial Maximum (LGM) regulated basin infilling on the scale of individual basins.

GEOLOGY OF THE STUDY AREA

Tectonic Setting

The Neogene tectonics of the Dinarides-Hellenides is characterised by NE-SW shortening (e.g., Cavazza et al., 2004) due to the northward motion of the Adriatic plate with respect to Europe (**Figure 1**).

The Western Kosovo Basin and Tropoja Basin are both located in the hanging wall of the main normal fault of the SPNF system (**Figure 2**). The stratigraphy of the Western Kosovo Basin is indicative of several cycles of internal drainage (e.g., Elezaj, 2012). The Black Drin River (**Figure 1**) traverses crust that underwent Mio-Pliocene exhumation and E-W extension (Muceku et al., 2008), as well as subsidence that included the deposition and preservation of Pliocene lake sediments (Lindhorst et al., 2014).

The SPNF and related faults coincide with a significant jump in elevation and slope angles (**Figure 2**). The maximum relief of ~2500 m occurs in the vicinity of the Tropoja and Western Kosovo Basins, where the Prokletije Mountains with peaks of ~2700 m are juxtaposed with the flat basins at only 200–350 masl

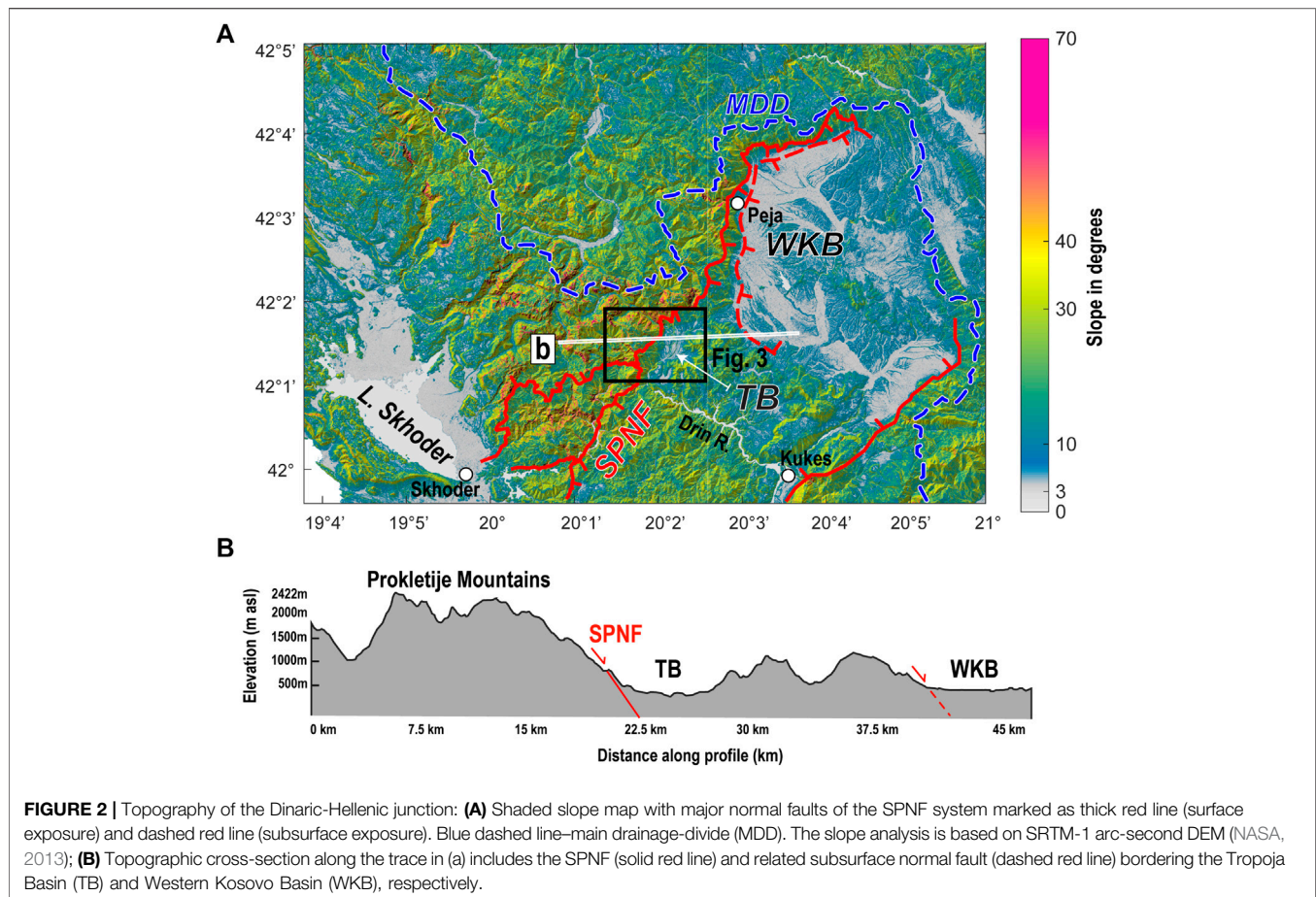


(Figure 2B). At the northern limit of the Western Kosovo Basin the relief decreases to ~1000 m.

The Topoja Basin is filled with ~400 m of Pliocene-Holocene sedimentary rock (Figure 4, Meço and Aliaj, 2000; Gjani and Dilek, 2010; Pashko and Aliaj, 2020). Three rivers (Valbona, Gashit and Bushtrices, Figure 3) carved the basin fill and generated three terraces (Figures 3, 4). We sampled the lower and intermediate terraces for terrestrial cosmogenic nuclide (TCN) dating (yellow stars in Figures 3A,B). The Valbona Valley hosts the principal river of the same name that drains the Topoja Basin. This uppermost part of this valley contains a niche rock glacier shielded by the topography of the Albanian Alps (Prokletije Mountains, Figure 2), a ~3 km high mountain range (Kuhlemann et al., 2009). The striking relief of the Albanian Alps has been interpreted to reflect differences in the erodibility of the rocks on either side of the SPNF, as well as possible activity of this fault (Handy et al., 2019). The Pliocene-Holocene fill of the Tropoja Basin unconformably overlies the West Vardar Ophiolites in the hanging wall of the SPNF (Figure 4).

Tropoja Basin Stratigraphy and River Terraces

The Tropoja Basin contains three lithostratigraphic units with subhorizontal bedding (units one to three in Figure 4; Pashko

and Aliaj, 2020). The bottom unit (Unit 1) is up to ~25–75 m thick and unconformably overlies the West Vardar Ophiolite. This unit contains layers of marls intercalated with medium- and coarse-grained sandstone (Figure 4C, Figure 5C). It has been dated as Late Pliocene using mollusk aggregations, pollen, and intercalated diatom-rich layers of marls (Gjani and Dilek, 2010; Pashko and Aliaj, 2020). We interpret this unit as a lacustrine deposit in a paleo-intramontane lake. At the Valbona River outlet, this unit onlaps the sub-ophiolitic mélange of the West Vardar Ophiolite and the Triassic limestone and Cretaceous flysch of the High Karst nappe (Figures 4A,B). The strata locally dip some 20° to the NW, i.e., towards the SPNF (Figure 5C). The very local nature of this dip and the lack of an increased layer thickness toward the SPNF precludes any fault-related rotation of the layers in the hanging wall of the SPNF. Instead, we attribute these unusual strata orientations to recent gravity sliding.

The intermediate unit (unit 2) is up to ~150 m thick and unconformably overlies unit 1 (Figure 4B). Unit 2 comprises clast-supported conglomerate with a sand-clay matrix and local coal seams (Figure 4C, Figure 5C). Coarse sandstone layers and light-grey carbonaceous conglomerates contain tractional sedimentary structures. We interpreted unit 2 as a fluvial conglomerate of Late Pleistocene-Holocene age (Pashko and Aliaj, 2020). Layers of unit 2 seal the SPNF at the outlet of

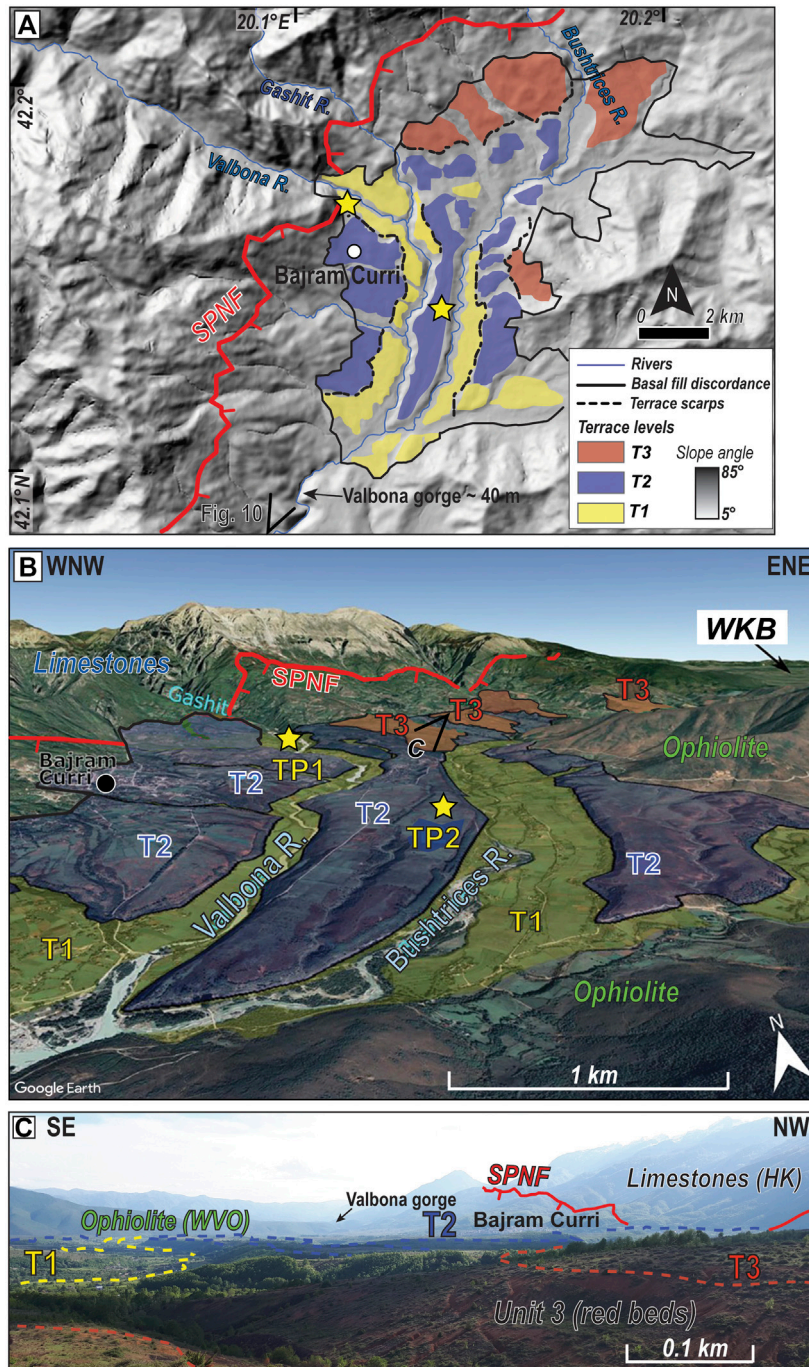


FIGURE 3 | Overview of fluvial terraces and abandoned river channels documenting episodic incision of the Tropoja Basin (TB) sediments: **(A)** Map with DEM hill shading and location of fluvial terraces. Terraces are numbered from youngest to oldest levels, T1 to T3. Thick red line—trace of the SPNF; Blue—present-day rivers in the TB; **(B)** Satellite image from *Google Earth* of the Tropoja Basin showing terrace surfaces coloured according to relative age. Imagery from *Google Earth*TM, 42° .18'N, 20°06'E, 7/01/2021. Yellow stars—location of ³⁶Cl depth profiles; **(C)** Pleistocene-Holocene fluvial terraces. Note hummocky “terra rossa” (red beds) of Unit 3 (foreground) and the high relief of the Albanian Alps (background right) in the footwall of the SPNF. WVO—Western Vardar Ophiolite; HK - High Karst Nappe.

Valbona (**Figure 4A**), indicating that little or no normal faulting has occurred since their deposition.

Unit 3 some 30–50 m thick occurs along the northern and the southeastern margins of the Tropoja Basin (**Figure 4A**)

and comprises lithologies ranging from reddish conglomerates, sandstones and red shales of presumably Holocene age (**Figure 5A**). Some of its units have weathered red. Red soils form by the autogenic dissolution

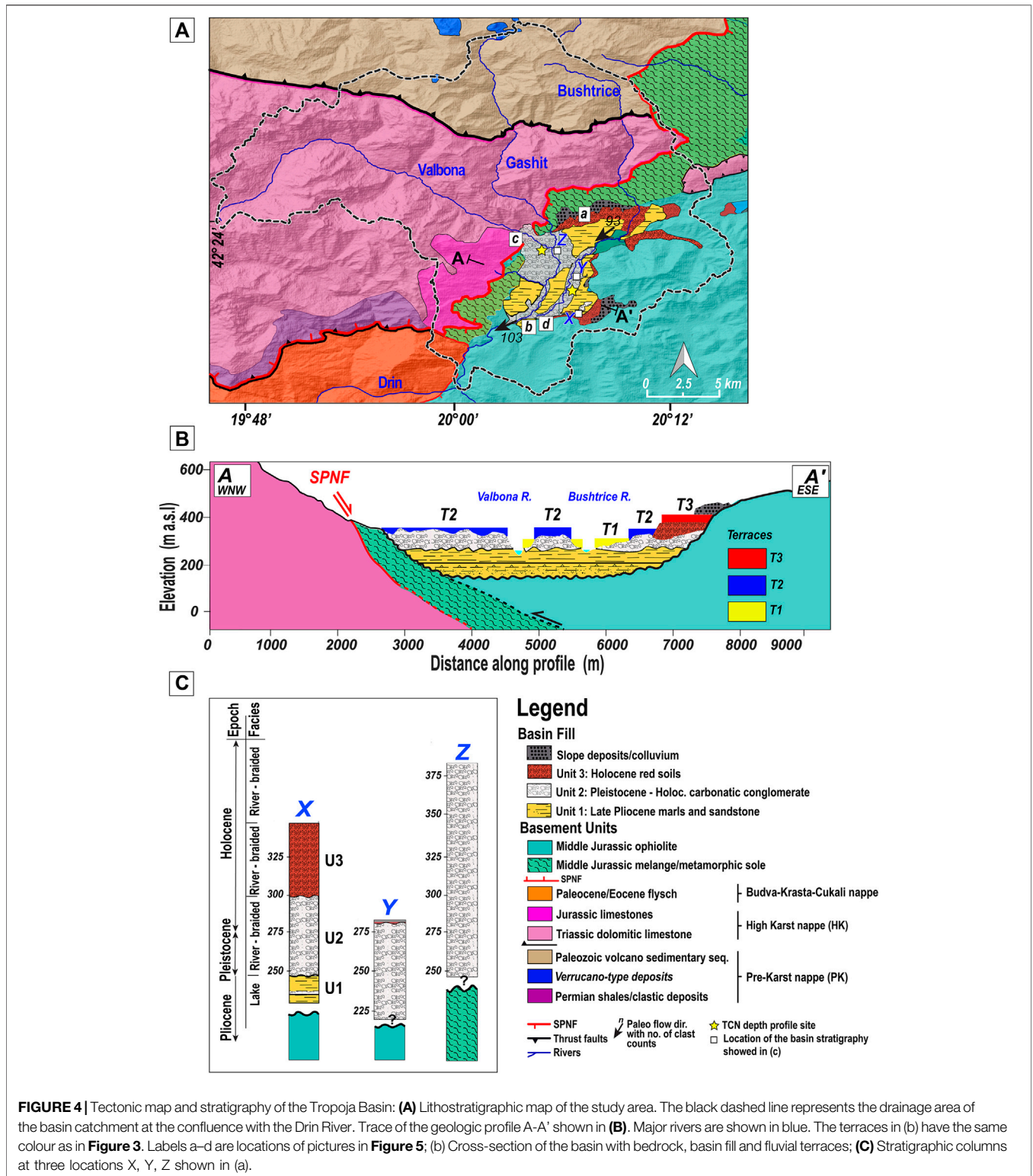


FIGURE 4 | Tectonic map and stratigraphy of the Tropoja Basin: **(A)** Lithostratigraphic map of the study area. The black dashed line represents the drainage area of the basin catchment at the confluence with the Drin River. Trace of the geologic profile A-A' shown in **(B)**. Major rivers are shown in blue. The terraces in (b) have the same colour as in **Figure 3**. Labels a–d are locations of pictures in **Figure 5**; **(b)** Cross-section of the basin with bedrock, basin fill and fluvial terraces; **(C)** Stratigraphic columns at three locations X, Y, Z shown in (a).

of carbonate and the possible addition of allochthonous aeolian sands commonly described in the Balkans as Terra Rossa (e.g., Muhs et al., 2010).

The bedding of all units is generally sub-horizontal with local variations due to gravity sliding. Measured dip and dip-directions of the clast imbricates in bedding of the

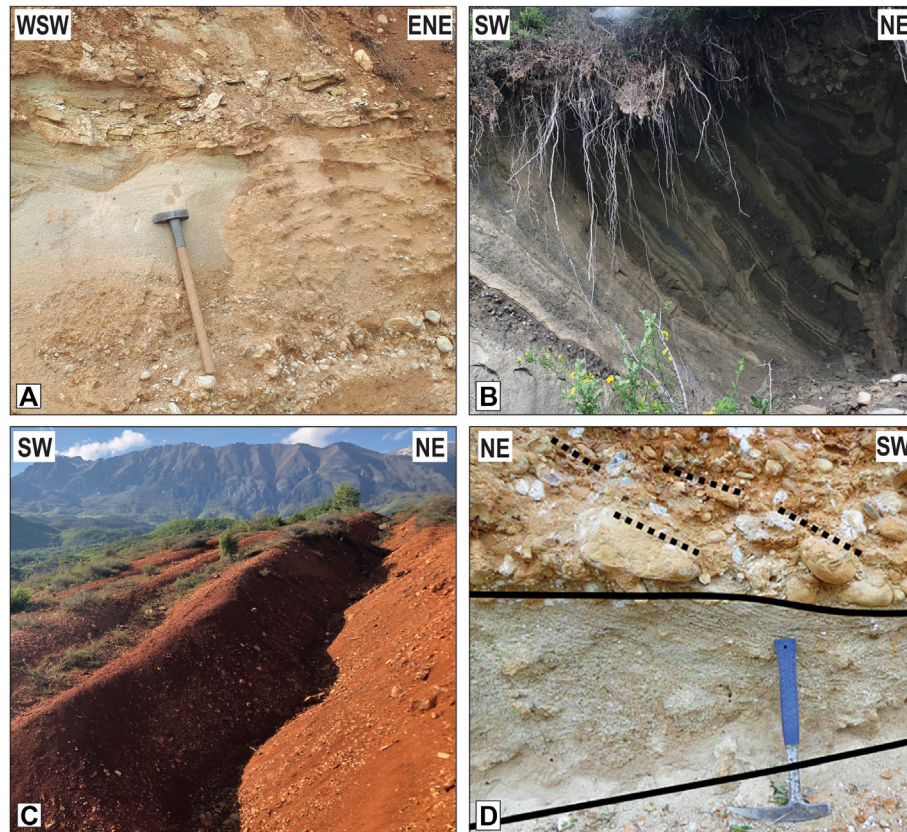


FIGURE 5 | Lithologies of the Tropoja Basin: **(A)** Unit 1: Grey marl and conglomeratic layers. The hammer is ~55 cm long; **(B)** Unit 1: grey marl and intercalated sandstone with bedding locally tilted to the NW; **(C)** Unit 3: Red beds (Terra Rossa) at the northern margin of the basin with layers of round pebbles; **(D)** Unit 2: Carbonate-rich conglomerate with inclined bedding overlying carbonaceous sandstone between black lines. Length of hammer ~33 cm. Locations of pictures labelled a–d in **Figure 4A**.

TABLE 1 | Results of the ^{36}Cl cosmogenic nuclide analysis.

Profile	Level	Lat. (N)	Long. (E)	Alt. m asl	EARL**	Mean	Median	Mode	Lowest χ^2	Max	Min
TP1*	T1	42.38	20.08	283	12	10.4 ka	9.7 ka	8.2 ka	17.3 ka	35.1 ka	3.7 ka
TP2*	T2	42.36	20.10	286	56	14.5 ka	13.9 ka	12.3 ka	15.5 ka	40.2 ka	5.8 ka
Incision rate (mm/yr)						10.7	10.4	11.7	24.4	8.6	20.9

*Labelled as TP1-N, TP2-S in the Supplementary Informations **EARL: Elevation above present-day river level (m)
Bold values are reported in the text.

carbonaceous conglomerate of unit 2 indicate river paleocurrent directions (dotted lines of **Figure 5D**). After correction, the paleocurrent direction is south-to southwest-directed (azimuth 120° , black arrows in **Figure 4A** and **Supplementary Figure S5**).

MATERIALS AND METHODS

^{36}Cl Depth Profile Dating

Terraces T1 and T2 in the Tropoja Basin were sampled for cosmogenic ^{36}Cl dating (Gosse and Phillips, 2001; Ivy-Ochs

et al., 2009) in two freshly excavated vertical terrace profiles, labelled TP1 and TP2 (yellow stars in **Figure 3**). TP1 is in the lowest terrace T1 at 283 m asl (**Table 1**) that incised unit 2 (**Figure 4B**) along the Valbona River. A total of six samples (500 g each) of conglomerate comprising carbonate components and calcite cement were collected at equal vertical intervals between depths of 50 and 250 cm. Samples were not collected near the surface to avoid disturbances of the depth profile by bio- or cryoturbation (e.g., Schaller et al., 2009). When sampling, care was taken to select well-rounded pebbles to ensure fluvial provenance and common pre-depositional history (**Supplementary Table S1** Supplementary Information). TP2

was sampled at 286 m asl in a freshly dug trench on terrace T2 on carbonate conglomerates of unit 2 (**Table 1**) following the same sampling procedure.

^{36}Cl dating was performed by the isotope dilution method (Ivy-Ochs et al., 2004; Ivy-Ochs et al., 2009). The samples were leached twice with 2 M HNO_3 for 24 h to remove meteoritic chlorine and an aliquot of ~ 10 g was separated for main and trace element analysis. The remaining sample material was dissolved with pure HNO_3 and spiked with 3.6 g of a ^{35}Cl carrier. Chlorine was precipitated as AgCl by adding AgNO_3 to the sample and then dissolved again in an NH_3 solution to remove sulfur as a precipitated BaSO_4 (Ivy-Ochs et al., 2004). Accelerator Mass Spectroscopy (AMS) analysis was performed at the Laboratory for Ion Beam Physics (LIP) at the ETH-Zurich following the procedure described by Christl et al. (2013). In addition to AMS measurements, we measured main and trace elements to correct the ^{36}Cl production rate (**Supplementary Table S2-Supplementary Information**).

We computed the depth profile age using Monte Carlo simulations in Mathcad (see Mair et al., 2019). Information about the inherited amount of ^{36}Cl before exposure and the age of exposure was obtained from ^{36}Cl concentration patterns for each depth profile (Hidy et al., 2010; Mair et al., 2019). The model was designed to compute depth-profiles of cosmogenic nuclide for a series of user input parameters. In the Monte Carlo routine, we accounted for the topographic shielding effect and inheritance of ^{36}Cl . The input parameters required by the algorithm and the values used are summarized in **Supplementary Table S3** of the Supplementary Information.

Topographic and Fluvial Analysis

We analyzed the river landscape at the Dinaric-Hellenic junction with two morphological measures: k_{sn} , the channel steepness index, as shown in **Figures 7A, Figure 9A** (Flint, 1974; Kirby and Whipple, 2001; Snyder et al., 2000) and χ (Chi), which we use as a proxy for fluvial-morphological stability in eroding and uplifting systems (Perron and Royden, 2013; Willett et al., 2014), as shown in **Figure 9B**. The channel steepness index, k_{sn} is a dimensionless parameter defined as:

$$k_{\text{sn}} = S/A^{-\theta} \quad (1)$$

where S is the local river gradient (taken to be positive in the downstream direction), A is upstream drainage area, and θ_{ref} is a reference concavity index (Wobus et al., 2006). Stated simply, k_{sn} tells us how much the channel steepness deviates from a reference concavity that is corrected for differences in drainage area. Faulting or lithological boundaries can cause steepness to deviate from θ_{ref} , such that the k_{sn} values will increase on the uplifting block and/or on the side of the fault with the more erosion-resistant bedrock. The higher the uplift rate and/or the more erosion-resistant the bedrock, the higher the k_{sn} -value and the greater the deviation from the reference concavity, θ_{ref} .

χ (Chi) has dimensions of length (m) and is defined:

$$\chi = \int_{x_b}^x \left(\frac{A_0}{A(X')} \right)^\theta dx \quad (2)$$

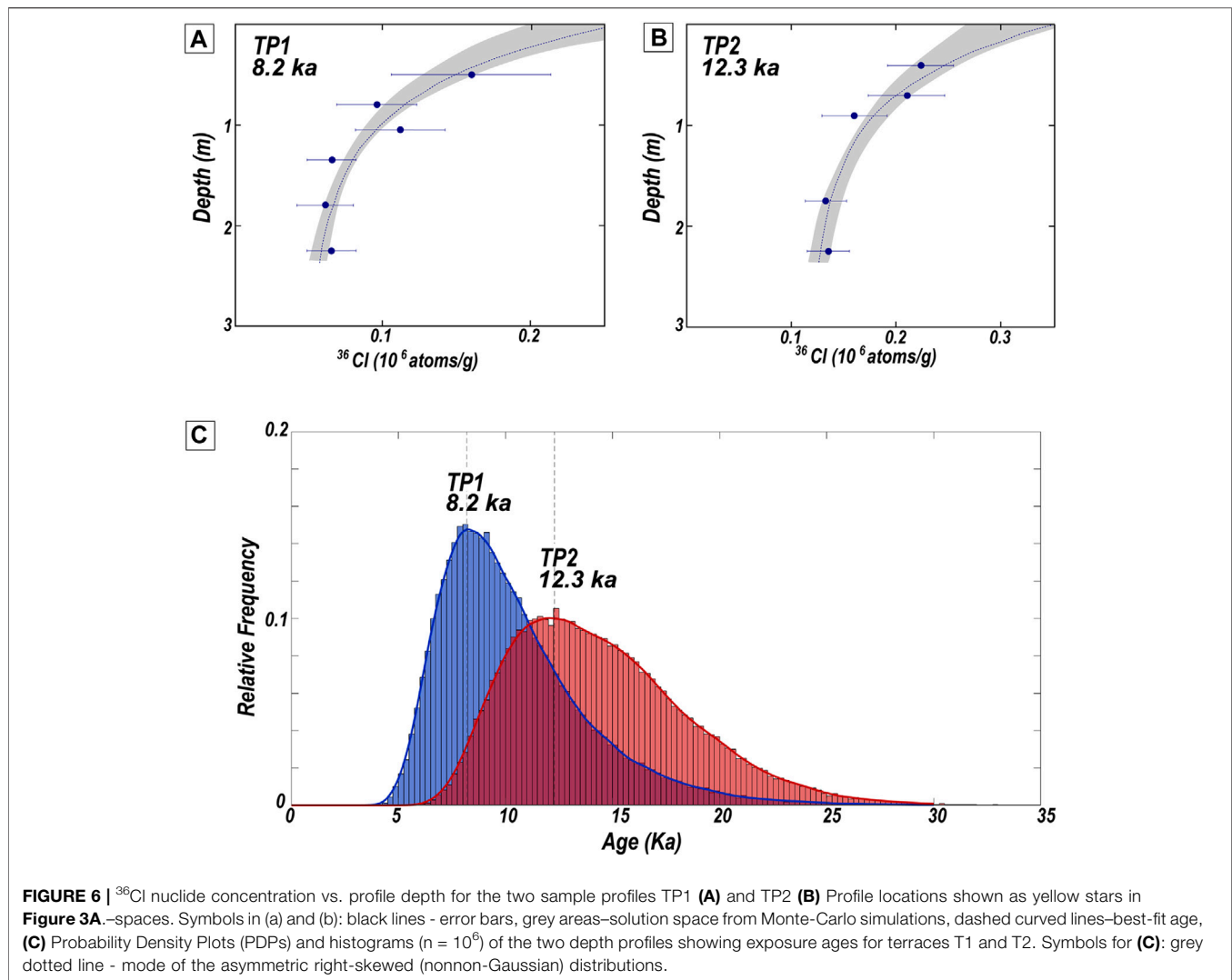
where A_0 is an arbitrary scaling area and the integration to obtain χ is performed from a base level at x_b to a location x upstream along the river channel. In our applications of χ below, the difference in χ values between river channels can be interpreted as an indicator for divide instability, provided that the uplift rate, climate, and rock erodibility are equal and that there are no major transients in river profiles (Willett et al., 2014). The river with the lower overall χ value has greater erosive potential than does the river with the higher overall χ value. χ maps like **Figure 9B** help visualize the direction that unstable drainage divides are expected to migrate (**Section 5.1**).

In **Section 5**, we use k_{sn} and χ maps (**Figure 9**) to assess how faulting, lithology, post-LGM climate and base level change have affected fluvial morphology at the scale of the Dinaric-Hellenic junction. The two parameters, k_{sn} and χ , are complimentary because k_{sn} is more sensitive to short-wavelength perturbations in the river profile, whereas χ better detects changes in regional steady state in the fluvial system, with the changes referring to a shift from an older steady-state condition to the current steady-state condition. A steady-state condition in the morphological sense refers to a combination of variables (base level, climate, lithology, uplift rate, bedrock characteristics) that are assumed to be invariant in time and space over the area considered.

k_{sn} and χ were extracted from a digital elevation model (DEM) at 30 m (1 arcsec) resolution (Shuttle Radar Topography Mission, SRTM). The analysis itself was performed using the MATLAB software package TopoToolbox version 2 (Schwanghart and Scherler, 2014; 2017). The stream network was obtained from the DEM using the D8 flow direction algorithm. Watersheds with an area of $\leq 10 \text{ km}^2$ (e.g., streams created by spring meltwater) were disregarded in order to avoid artefacts at the low resolution of the DEM (30 m). We calculated the reference concavity (θ) using a Bayesian optimization of θ with the *mnoptim* function described in TopoToolbox (Schwanghart and Scherler, 2017). A reference value of $\theta_{\text{ref}} = 0.423$ was used for the part of the Dinaric-Hellenic orogen in **Figures 7, 9, 10**.

Knickpoints are defined as points or zones (knickzones) of abrupt change in the slope of rivers (e.g., Whipple and Tucker, 1999; Kirby and Whipple, 2012). Knickpoints can be identified either in plots of elevation vs. horizontal distance constructed from DEMs (e.g., **Figure 8C**) or in plots of elevation vs. χ (e.g., **Figure 7B**). Although elevation-distance plots are easier to grasp at first glance, the advantage of elevation vs. χ plots is that knickzones appear as morphological deviations from a steady-state river profile (Royden and Perron, 2013; Neely et al., 2017). We identified knickpoints with a preprocessing routine described in Schwanghart and Scherler (2017).

For the Drin River analysis in **Figure 8**, we used a tolerance value of 124 m calculated as the difference between filled and incised channels with a minimum uphill area of 15,000 pixels ($= 13.5 \text{ km}^2$). This high



tolerance value allowed us to identify knickzones in a large catchment area (e.g., Figures 8C, Figure 10). Knickpoints in the much smaller Tropoja Basin catchment were calculated with a lower tolerance value of 60 m. Anthropogenic knickpoints, for example, dams along the Drin, were not considered in any of the analyses.

RESULTS

Terrace Exposure Ages From the ^{36}Cl Depth Profiles

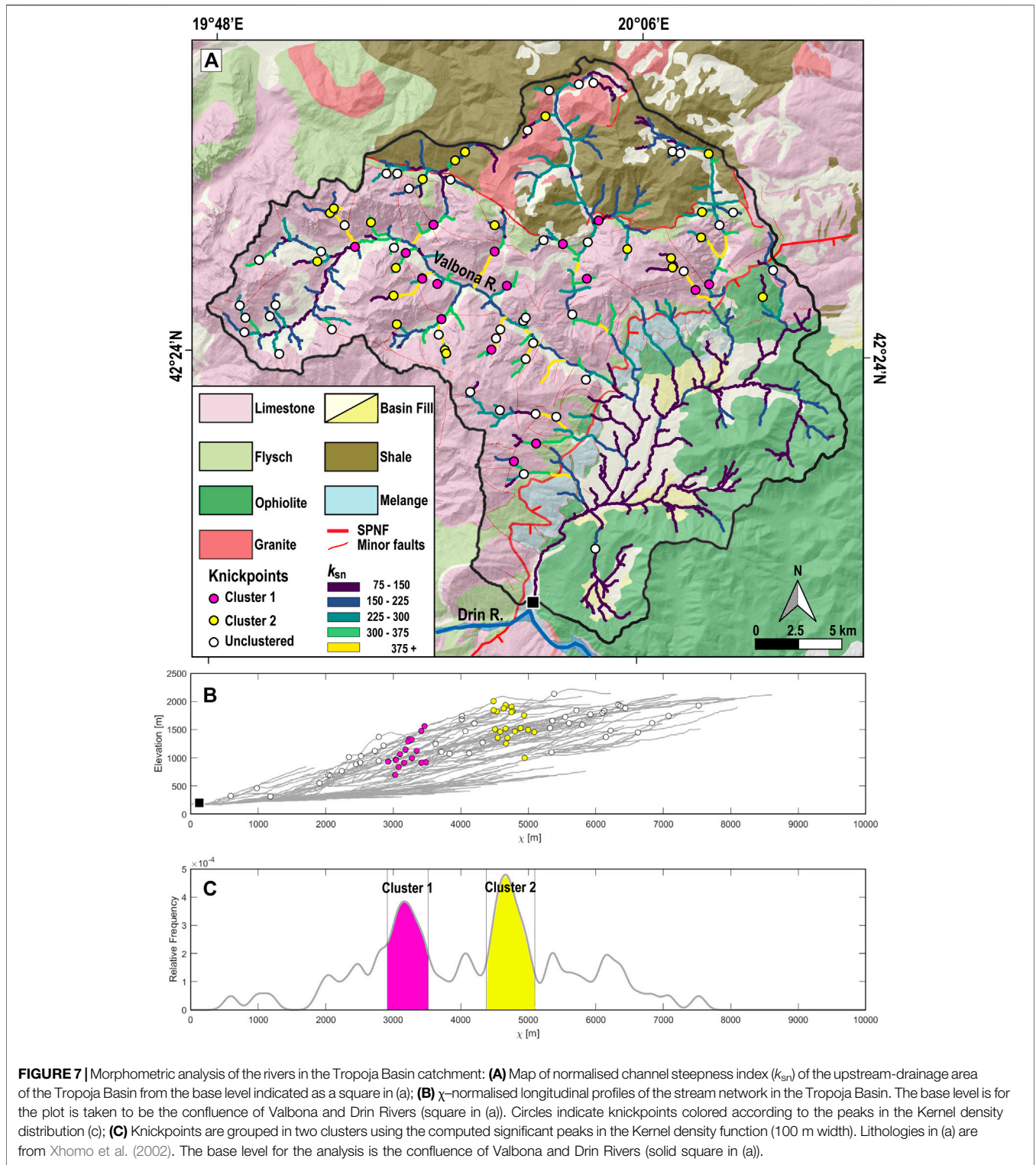
The two sampled terrace profiles, TP1 and TP2, show an exponential decrease of ^{36}Cl concentration with depth (Figures 6A,B) that allows us to estimate the erosion/incision rates (e.g., Gosse and Phillips, 2001). Probability Density Plots (PDPs) showing frequency vs. age have right-skewed distribution curves (Figure 6C). We chose the modal value instead of the mean as the best-fit exposure ages of ~8.2 ka and ~12.3 ka for terraces T1 and T2, respectively (dotted grey lines in Figure 6C and Table 1). The ages overlap within error. The age errors are

mainly due to uncertainties related to the neutron capture production rate.

The interested reader is referred to Section 1.4 of the Supplementary Information for a description of the method used to calculate river incision rates. We compared the minimum, maximum, and modal ages, which resulted in a best-fit incision rate of 11.7 mm/yr (Table 1). This value is assumed to be the best approximation of the fluvial incision rate of the Valbona River into the Tropoja Basin sediments during Late-Pleistocene to Holocene time.

Results of the Geomorphic Analysis

Most of the 80 knickpoints in the Tropoja Basin (Figure 7) do not coincide directly with significant lithological contacts along the SPNF, e.g., between the High Karst (HK) carbonates and the more erodible Cretaceous flysch and ophiolitic mélange (Figure 7A; Supplementary Figure S3). They also do not cluster along the SPNF itself (Figure 7A). This suggests either that they have migrated upstream since the most recent activity of the fault or that they reflect reconfiguration of rivers within the



drainage system and the establishment of a new steady state. Yet another possibility is that they reflect a fall in the base-level of the entire system (e.g., lowering of the Adriatic Sea).

A striking feature of the knickpoints in the Tropoja Basin is that about half of them cluster at two distinct intervals in the elevation vs.

χ plot with respect to the basin outlet (**Figures 7B,C**). The outlet is taken to be the confluence of the river draining the basin with the main trunk of the Drin River (solid square in **Figure 7A**). These clusters are coloured pink (first cluster) and yellow (second cluster) in the longitudinal profiles and kernel distribution in **Figures 7B,C**.

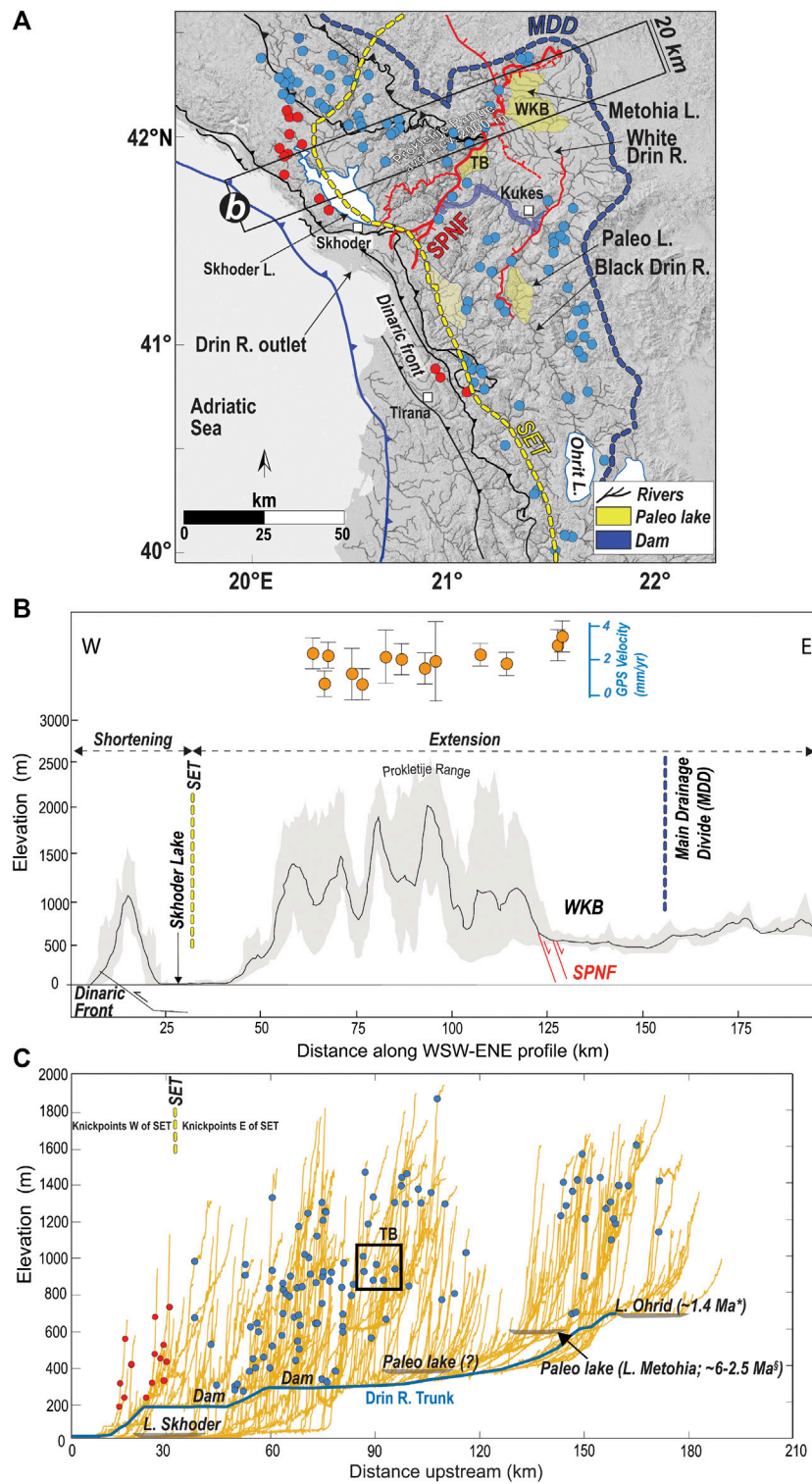
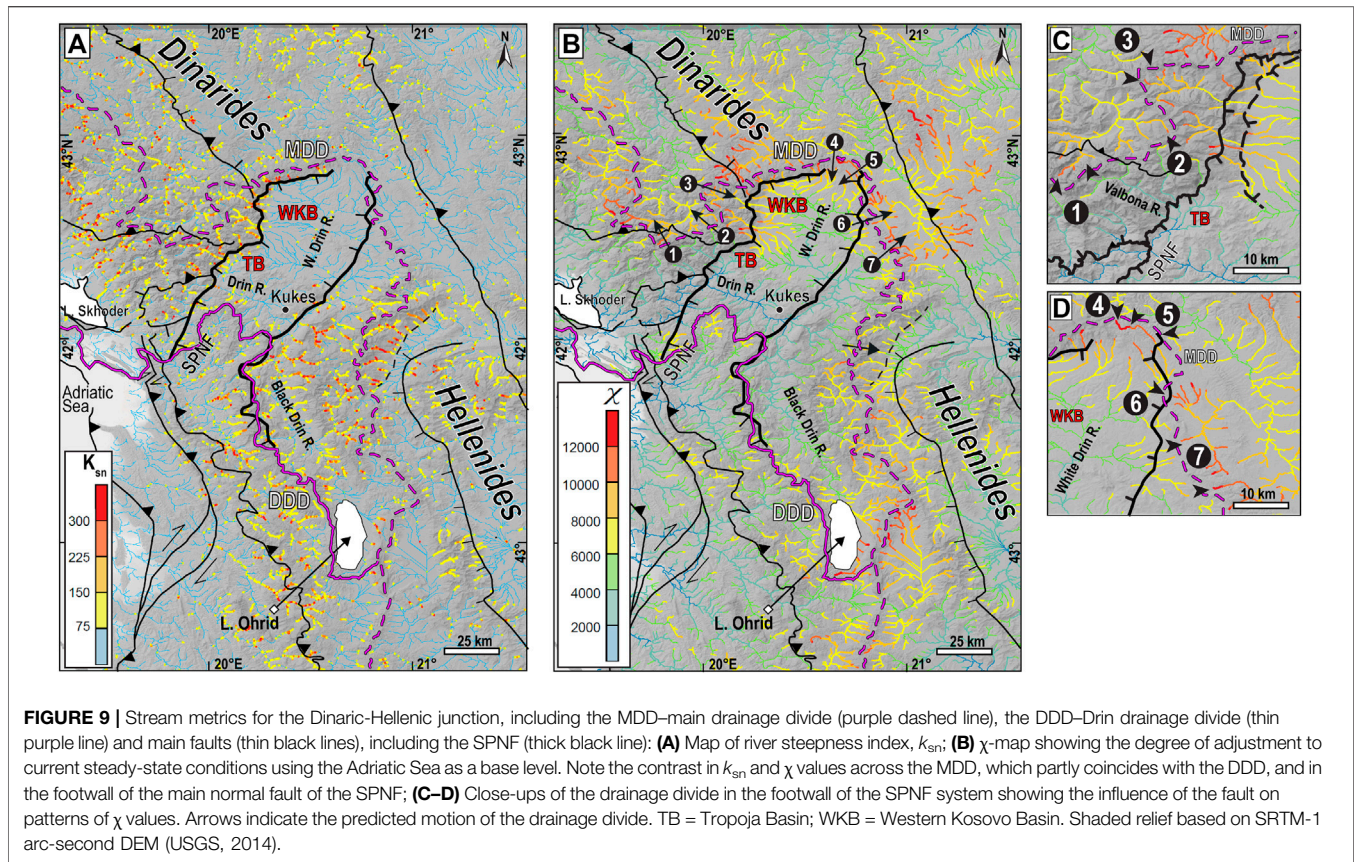


FIGURE 8 | Distribution of knickpoints and relief (defined as the difference between the min and max elevations) at the Dinarides-Hellenides junction: **(A)** Hillshade map based on SRTM-1 arc-second DEM (USGS, 2014); Additional elements are river streams (black lines), the trace of the shortening-extension transition (SET–yellow dashed line), main drainage divide (MDD–blue dashed line). Knickpoints to the west and east of the SET are colored, respectively, red and blue. The base-level is the outlet of the Drin River into the Adriatic Sea as labelled in (a); **(B)** 20-km wide swath profile with maximum and minimum elevations at upper and lower boundaries of the grey area, respectively. The mean elevation is represented as a solid black line. Faults - normal (red) and thrust (black). GPS velocities given in mm/yr (orange dots) with their relative errors as a vertical line. GPS data in (b) are from D’Agostino et al. (2020); **(C)** Longitudinal river profiles and locations of knickpoints identified in (a), 0 km on the x-axis is the Drin River outlet, the reference level used in the calculation of knickpoints. Paleo-lakes are indicated as grey polygons. Age estimates of Lake Ohrid (~1.4 Ma-to-Present) taken from Wagner et al. (2019) and of the paleo-Metohia Lake in the Western Kosovo Basin (WKB) from Neubauer et al. (2015b).



Many of them coincide with changes in k_{sn} values, as shown by the colours along the streams in **Figure 7A**. The other knickpoints (white dots) are scattered across the drainage area. We discuss scenarios for their origins in the *Landscape morphology, terraces and climate*.

To compare the fluvial metrics of the Tropoja Basin catchment with the regional drainage network, we identified a total of 114 knickpoints in the entire Drin River drainage basin, starting from the Drin River outlet (taken here to be the base level, **Figure 8A**) to elevations between ~190 and 1850 m asl (**Figure 8B**). These are coloured red and blue depending on their location with respect to the dashed yellow line marked SET for the transition from orogen-normal shortening to extension. We note that the knickpoints in the Drin drainage system in **Figure 8A** include six points in the Tropoja Basin catchment (labelled TB in **Figures 8A,C**).

Overall, channel slopes are much steeper along the Adriatic coastal mountain range where shortening is ongoing than in the high-relief Dinaric hinterland where the orogen is actively extending. There, the horizontal displacement rates range from 1.5–4 mm/yr normal to the strike of the orogen (**Figures 8B,C**, D'Agostino et al., 2020). The knickpoints identified in the coastal range (red dots in **Figure 8C**) are much more closely spaced than in the hinterland (blue dots in **Figure 8C**). Most knickpoints occur where rivers flow from the high relief of the carbonate rocks forming the Dinaric nappes (**Figure 1**) to alluvial plains underlain by Neogene sediments (**Figures 8A,B**). These are located

80–200 km upstream of the Drin outlet and are interpreted as paleo-lakes, as labelled in **Figure 8C** and discussed in the next chapter.

Two features of the distribution of blue knickpoints stand out in the channel profiles in **Figure 8C**: 1) At distances of ≥ 90 km from the Drin outlet, a gap in slope between 1,000 and 1,300 m asl separates a group of points above 1,300 m asl from the rest of the points below. This gap corresponds generally with a flat segment of the Drin River trunk at 300–400 m asl that is labelled paleo-lake in **Figure 8C**; 2) At distances closer to the Drin outlet (<90 km), the blue knickpoints occur at a broad range of elevations between 300 and 1,400 m. The relationship of the knickpoints and their elevation to paleo-lakes is discussed below in section 5.1.1.

The k_{sn} and χ -maps in **Figure 9** for the entire fluvial network of the Dinaric-Hellenic junction show that the footwall of the SPNF and its related faults coincide with of the highest values of both parameters. Here, it is important to note again that the SPNF juxtaposes contrasting lithologies, from limestone rocks of the Dinaric nappes in its footwall to ophiolite and sub-ophiolitic mélange of the West Vardar Ophiolites in its hanging wall (see **Supplementary Figure S1**). Lower k_{sn} values characterize the graben between the conjugate normal faults of the SPNF system, as well as along the Adriatic coast west of the SET (blue colors in **Figure 9A**).

Bright colors in **Figures 9B–D** indicate four parts of the river network that are not in steady-state and where drainage divide mobility is highest: 1) the northern and eastern borders of the Drin catchment along the SPNF system towards the hinterland; 2) along the White Drin in the north; and 3) along the Black Drin in the east, as well as 4) in the vicinity of Ohrid Lake. The northwestern part of the Drin catchment is also in a transient state as indicated by the contrast of χ -values on either side of the drainage divide (**Figures 9B,C**).

DISCUSSION

The overarching question posed when interpreting our data is: How are patterns of deposition and erosion linked on different scales? To answer this, we begin with the scale of the Drin River catchment, then progress to the smaller scale of the Tropoja Basin, where the record of sedimentation and fluvial incision is best preserved and can be assessed in the context of faulting, climatic variation, stream-capture and autogenic factors, e.g., events that occurred within the basin.

Regional Drainage Pattern and Its Controls

Several important points emerge from the river stream metrics at the scales of the Tropoja Basin (**Figure 7**) and the Dinaric-Hellenic junction (**Figures 8–10**). On the orogenic scale, we observe that both k_{sn} and χ -values are higher in the footwall of the main normal faults making up the SPNF system (thick black lines in **Figure 9**). These high values indicate that the fluvial network is still adjusting to rock uplift and variable erosion along and across the SPNF system. This is particularly evident by the jump in k_{sn} values along an E-W trending segment of the SPNF forming the northern border of the Western Kosovo Basin (**Figure 9A**). This may indicate ongoing activity of that part of the fault. Another potentially active fault scarp can be identified in the k_{sn} map in the hanging wall of the large low-angle normal fault located just east of the main drainage divide (thin dashed black line in **Figure 9A**, from Dumurdjanov et al., 2020). Alternatively, the difference in k_{sn} values between the bed channels in carbonate-rich rocks (High Karst and Pre-Karst units) and ophiolitic, silico-clastic and metamorphic rocks (Western Vardar Ophiolites and associated nappes) (**Figure 1, Figure 9A, Supplementary Figure S1**) may be attributed to water runoff, infiltration, and chemical dissolution in the carbonate-rich bedrock (e.g., Central Apennines, Tucker et al., 2011). Chemical dissolution of carbonates and water infiltration can lower the bed of the channel, altering the channel's steepness that, in turn, increases the response time to climate and tectonic forcing, steepening the topography in karstified areas (e.g. Ott et al., 2019).

A further striking feature is that the χ values are generally highest in the narrow domain between the SPNF and the main drainage divide (MDD in **Figure 9B**, and close-ups c, d). This suggests that this domain is not in equilibrium with the current steady-state conditions. We note that these locally high χ values occur against a background of heightened χ values across the entire Dinaric-Hellenic chain, indicating substantial migration of

fluvial divides on the scale of the orogen. This is especially evident at the White Drin outlet into the Western Kosovo Basin (arrows in **Figure 9B**). Interestingly, the Western Kosovo and Tropoja basins both show very low k_{sn} values and low-moderate χ values (**Figures 9A,B**), in keeping with the observation that they are relatively flat, uplifted domains with little ongoing erosion (see white areas in the slope map, **Figure 2A**).

Following Willett et al., 2014, we interpret the asymmetry of χ values on either side of the main drainage divide and the SPNF in **Figure 9B** to indicate that in most places, the divide is migrating away from the fault (black arrows in **Figure 9B**). Only at the N and NE end of the SPNF do the χ values indicate that the divide is migrating to the SW, i.e., into the graben between the two normal faults (**Figures 9C,D**).

The confluence of tributary channels delineates the trunk of the Drin River (**Figure 8B**) and defines flat river segments on its way to the current outlet at the Adriatic Sea (**Figure 8C**). These segments partly coincide with Plio-Pleistocene deposits like those found at Lake Ohrid (**Figure 8A**). We therefore interpret these flat segments as paleo-lakes in the sense of Whittaker and Boulton (2012) (**Figures 8A,C**). A good example of such a paleo-lake is Lake Metohia, which occupied part of the Western Kosovo Basin during Pliocene to Early Pleistocene time (Neubauer et al., 2015b; location in **Figure 8A**). These paleo-lakes probably formed prior to river-capture events, as proposed below in chapter 5.

There are no discontinuities in stream profiles and river metrics across the transition from active extension to shortening (SET in **Figure 8C, Figure 9A**), indicating either that this transition is not sharp or that the rate of river incision is high with respect to the current strain-rate of the crust. Along the Adriatic coast where thrusting and shortening are ongoing (**Figure 1, Figure 8A**), the streams have steep sides and clustered knickpoints (red dots in **Figure 8C**). This is interpreted to reflect the ongoing adjustment of the streams to tectonically induced uplift.

Knickzones away from the Adriatic coast and situated east of the SET within 90 km of the Drin outlet at elevations from 300 to 1,400 m asl (**Figure 8C and Section 3.2**) probably reflect older events. It is tempting to attribute the lowest ones between ~200 and 400 m to base-level fall during the lowering of the Adriatic Sea by some 120 m during the LGM (Pirazzoli, 1991; Lambeck and Purcell, 2005). Points above 400 m asl may well be older. Some of the knickpoints may be related to downcutting in the immediate aftermath of Messinian drainage of the Mediterranean Sea (Garcia-Castellanos and Villaseñor, 2011). However, most of the rivers adjoining the N-S directed Black Drin River may have not drained in the Adriatic Sea at that time as they were part of an internally drained systems (see chapter 5). Others may reflect one or more episodes of regional uplift associated with extension in the upper plate of the retreating and delaminating Adriatic slab (e.g., Matenco and Radivojević, 2012; Unen et al., 2018).

The gap in knickpoints identified in **Figure 8B** further away from the Drin outlet and within the Dinaric hinterland at elevations between 1,200 and 1,600 m asl is enigmatic inasmuch as it coincides with the lateral extent of a flat

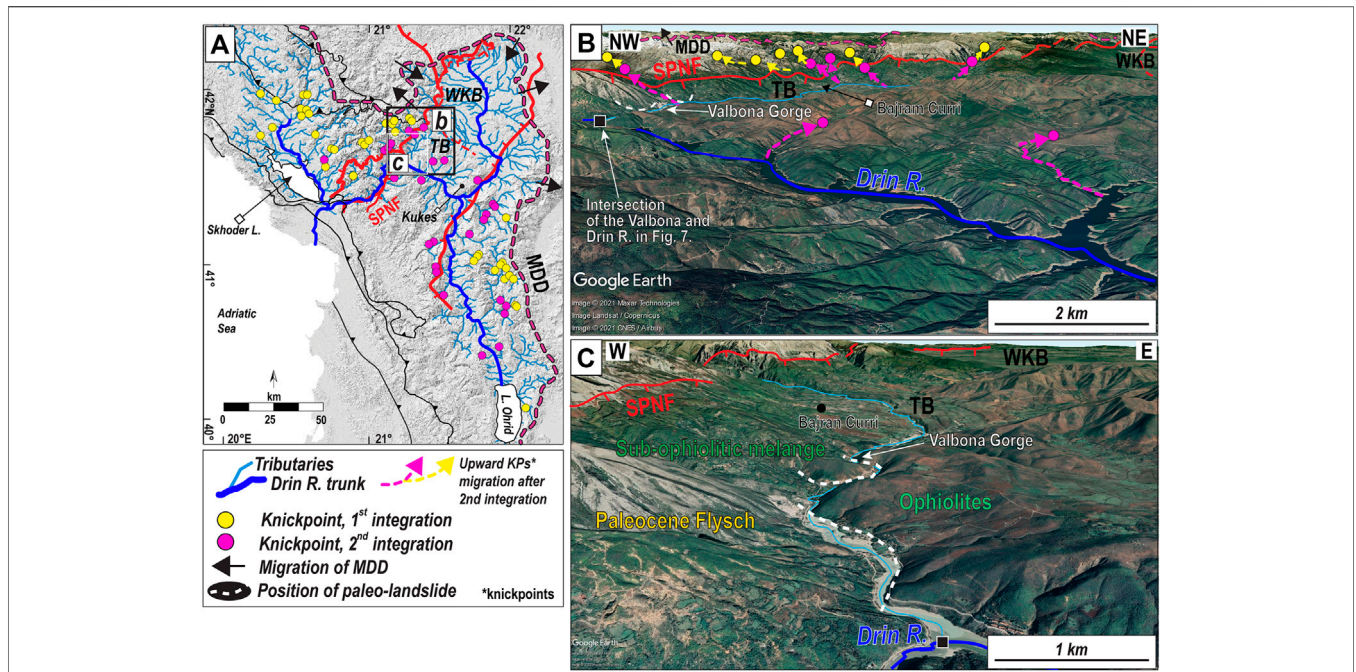


FIGURE 10 | Knickpoints along rivers in the Drin catchment: **(A)** Two knickpoint generations as a function of distance from the Drin River trunk (blue stream): first generation—yellow dots, second generation—pink dots, as in **Figure 7**. Youngest knickpoints coloured red in **Figure 8** are not shown here. Black arrows indicate the predicted migration direction of the main drainage divide (MDD) as shown in **Figure 9B**; **(B)** Bird’s-eye view of the two generations of knickpoints in the vicinity of the Tropoja Basin (TB). Pink arrows—migration direction of second generation of knickpoints; Yellow arrows—upstream migration direction of first knickpoint generation followed by second integration of the Drin River (see text for explanation); **(C)** Bird’s-eye view of the Valbona gorge and intersection with the Drin River trunk. Dashed white lines indicate the possible location of the former toes of paleo-landslides that may have dammed the Valbona River downstream of the TB. These are based on a qualitative analysis from *Google earth* and from the landslide inventory map of Albania (Jaupaj et al., 2017). Images from *Google Earth*TM, 42° 13'N, 20° 11'E, 7/22/2021.

segment of the Drin River trunk (**Figure 8C** and **Section 3.2**). One explanation is that this gap may be an artifact of projecting river channels in the high Albanian Alps far to the north (e.g., north of the Western Kosovo Basin) into the same section as the Drin River trunk. Rivers with these high-altitude knickpoints only join the Drin River after traversing the mountains from north to south, perpendicular to the plane of the section in **Figure 8C**. Alternatively, these high slope knickpoints formed during normal faulting along segments of the SPNF along the northern limit of the Western Kosovo Basin (**Figure 2A**, **Figure 9A** and discussion above); these knickpoints have since migrated into the footwall of the SPNF.

Landscape Morphology, Terraces and Climate

Today, we see that the Tropoja Basin is adjusted to the current steady-state conditions (**Figures 9A,B**), as indicated by low χ values from the outlet of the Adriatic Sea to the Tropoja Basin and within the Drin River up to the vicinity of the town of Kukes. Large parts of the Western Kosovo Basin and the Black Drin River are not adjusted to the current steady-state conditions (high χ -values in **Figure 9B**) with respect to the current base-level represented by the Adriatic Sea.

We focus our analysis on the Tropoja Basin as it gives us the opportunity to relate incision events and knickpoint migration to

dated terrace levels. This in turn provides a potential age for catchment-wide reorganization events. To do this, we first identify mobile knickpoints, defined as knickpoints that migrate upstream due to a downstream perturbation (e.g., base-level fall, Crosby and Whipple, 2006). Assuming that the confluence of the tributary streams and the Drin River trunk (the base-level reference, $\chi = 0$ in the χ -plots of **Figures 7, 10**) were stationary while the knickpoints migrated upstream, we computed knickpoints scaled to an upstream drainage area (e.g., Crosby and Whipple, 2006; Berlin and Anderson, 2007; Marrucci et al., 2018; Schwanghart and Scherler, 2020). In catchments with uniform erodibility and precipitation, the knickpoint migration celerity (V) scales with tributary drainage area (A):

$$V = CA^p \tag{3}$$

where C and p are constants fitted to the data (Crosby and Whipple, 2006). The drainage area (A) is integrated over the river distance to produce variable χ and points with the same contributing drainage area in the river network plot at the same value of χ . As the propagation velocity of the signal is proportional to the upstream drainage area, each knickpoint propagating upstream from the basin outlet (black square in **Figure 7A**) has a similar value of χ . The 71 knickpoints in **Figure 10** are interpreted to reflect pulses of change in steady-state conditions that are migrating upstream. Local base-level changes in the fluvial system due to regional uplift or sea-level

change can trigger discrete waves of fluvial incision that cause knickpoints to propagate upstream (e.g., Wobus et al., 2006; Berlin and Anderson, 2007; Kirby and Whipple, 2012; Schwanghart and Scherler, 2020). During this process, rivers can add new channels to their fluvial network (Stokes et al., 2002).

During the LGM the regional base level of the Drin was the Adriatic Sea at ~120 m below present-day sea level (Pirazzoli, 1991). However, from ~21 ka, sea level began rising in the Mediterranean Sea to its present level (Lambeck and Bard, 2000). This sea-level rise was not linear, but fluctuated, with two major changes in the rate of sea level rise at ~12 and ~8 ka. At these times, sea-level rise in the Mediterranean slowed significantly for several thousands of years before accelerating again. Interestingly, these periods coincide with the times of formation of T1 and T2 terraces in the Tropoja Basin (Figure 6). Unfortunately, no age exists for the oldest terrace level T3, that however must be older than 12 ka and likely is related to the lowest sea level during the LGM.

We propose that a new steady-state condition was established each time the sea-level rose significantly, thus creating an incision event or knickpoint that migrated upstream to adjust the river network to the new base level. These knickpoints are seen throughout the catchment of the Drin River (Figure 10, yellow and pink dots). The youngest incision event and related knickpoints (second generation, pink knickpoints) are related to the adjustment to the current steady-state condition and present base level of the Adriatic Sea. Based on the age of terrace T1, we interpret this incision event to be younger than 8 ka. Today, we infer from the low χ values in the footwall of the SPNF in the Tropoja Basin (Figures 9B,C) that the wave of incision passed through the basin and reached the hanging wall of the SPNF as indicated by the high χ values there (clusters of pink and yellow colored knickpoints in Figures 7A,B, respectively). On their way upstream, the migration of the knickpoints was significantly slowed because faulting along the SPNF juxtaposed erosion-resistant limestones of the High Karst Nappe with more erodible marls and shales in the sub-ophiolitic mélange of the West Vardar Ophiolite. This is also reflected by the higher values of k_{sn} in the limestone units of the High Karst nappe (HK in Figures 1, Figure 3C; Supplementary Figure S3) and other Dinaric nappes (Figure 9A). We speculate that an older pulse of incision and corresponding knickpoints (yellow dots and cluster in Figure 7) was related to an increase in the rate of sea-level rise between 8–12 ka, resulting in a renewed change in base level (Figure 10, first generation knickpoints, yellow dots). This first generation of knickpoints is still visible in the upper reaches of the Valbona and Drin Rivers, indicating that these rivers have not yet adjusted to the current steady-state conditions (Figure 10). The incision age is again bracketed by our terraces T1 and T2 to have occurred sometime between 8 and 12 ka.

The numerous knickpoints in the Tropoja Basin that did not form a χ cluster (white dots in Figures 7A,B) cannot be attributed to any major geological features (lithological boundaries, faults) or downstream changes in drainage. They may reflect minor local structures, for example, joints in the karstified limestones making up the High Karst nappe.

We tentatively correlate the age of terrace T3 with the lowest base-level during the LGM. However, we were unable to date this terrace and its age and origin remain speculative.

Climate is a factor that can control the river network as expressed by river metrics (e.g., Wobus et al., 2006; Kirby and Whipple, 2012). At the Dinaric-Hellenic junction and surrounding area, paleo-environmental multi-proxy data show a climate characterized by seasonally variable precipitation since the Plio-Pleistocene (Lacey et al., 2016; Wagner et al., 2019) with a slight increase in summer precipitation during the Younger Dryas cold event (~12.3 ka) and the temperate periods (Bordon et al., 2009). Alternating glacial and interglacial periods have a clear impact at the local scale of individual drainage systems, with increases or decreases in sedimentation rates that may have occurred independently of tectonic activity along the SPNF system (e.g., terrace aggradation vs. terrace incision; Pazzaglia, 2013). This is evident in the stratigraphy of the Tropoja Basin, where lacustrine sediments were covered by coarse-grained fan-type clastics long after tectonic activity on the SPNF ceased (Figure 4 and discussion in *Landscape morphology, terraces and climate*).

Fluvial terraces contain information about climatic fluctuations (Tucker and Slingerland, 1997; Macklin et al., 2002; Pazzaglia, 2013). The onset of humid-air circulation during glacial-interglacial cycles in the Mediterranean region led to a transient climate after ~1.36 Ma (Lake Ohrid climatic proxies, Wagner et al., 2019) linked with increased sedimentation rates (i.e., Ohrid Lake Figure 1; Vogel et al., 2010a; Wagner et al., 2012; Macklin et al., 2002; Carcaillet et al., 2009). Despite the significant error of our ^{36}Cl ages (Figure 5; e.g., Hidy et al., 2010), the modal ages of ~12 ka and ~8 ka, respectively, from the intermediate and lowest terraces in the Tropoja Basin (TP1 and TP2 in Figure 3) both fall within post-LGM time (Hughes, 2007). Late-Pleistocene glaciation (Würmian phase) in the highest elevation of the Prokletije mountains (Albanian Alps) is documented by moraines that occur down to ~1,000 m asl (Hughes, 2009; Milivojević et al., 2008—see also Supplementary Figure S3 in the Supplementary Information). Melting of cirque-type glaciers leading to more intense precipitation at these latitudes began after the Younger Dryas at ~12 ka (Wagner et al., 2019), followed abruptly by a short (~10² yrs) regional cold phase at 8.2 ka (Alley and Ágústsdóttir, 2005) when the climate was locally drier. These periods correspond with an overall increase in erosion during cooler phases in the northern hemisphere during the Cenozoic (Hermann et al., 2013). We infer that these climatic events also affected the upper reaches of the rivers, increasing sediment supply to the Tropoja Basin through the fluvial river network. This increased sediment supply together with the decreased rate of sea-level rise were conducive for the formation of terraces in the Tropoja Basin. The terrace morphologies (Figure 3) indicate that T1 occurs within an entrenched channel, whereas T2, and possibly T3, mark the inset of a broad alluvial plain sediment formed by a braided river system (unit 2 and planar morphology in Figures 3, 4 and Supplementary Figure S5). The interpretation that T2 was incised after the inset of braided river system is consistent

with the idea that the river had reached its transport capacity for sediments. Immediately after abandoning terrace level T2, the Valbona River started to cut down, forming an entrenched channel in T1. River entrenchment can reduce lateral river migration, leading to bank collapse (Malatesta et al., 2017). In turn, limited lateral mobility of the river increases vertical incision. Thus, the onset of river entrenchment can initiate a positive feedback that leads to yet more incision due to the concentration of stream power within a narrower bed (Malatesta et al., 2017). We propose that T1 may have resulted from bank erosion. Other factors to consider for the formation of the terraces in the Tropoja Basin are landsliding and damming of the Valbona River. Meltwater and increased runoff, possibly combined with earthquakes (e.g., Muço, 1995; Muço et al., 2012), would be expected to trigger slope instability in the form of landslides and debris flows that suddenly entered the drainage system (Stock and Dietrich, 2006; Marc et al., 2015). The 6.4 M_w 2019 Dursi event or 7 M_w 1905 Skhodra earthquake (Caporali et al., 2020; D'Agostino et al., 2020) are only two recent examples of active seismicity at the Dinaric-Hellenic junction. We speculate that at the outlet of the Tropoja Basin, the Valbona River may have been dammed by landslides that filled a narrow gorge of ~40 m depth (e.g., Jaupaj et al., 2017; dashed white lines in **Figure 10A**). Episodic damming could have favoured the creation of the terraces in the Tropoja Basin.

In comparing our estimated incision rates for the Tropoja Basin (**Table 1**) with the ^{10}Be -based incision rates for central and southern Albanian river terraces during the LGM and post-LGM periods, we find that the latter (~1.4 mm/yr, e.g., for Osum River terraces T7 and T8; Carcaillet et al., 2009) are ten times lower than the ~12 mm/yr that obtained here for the ~12–8 ka interval between terraces T2 and T1 (**Table 1**). This difference can be explained either by greater precipitation in northern Albania or by the migration of the knickzone through the Tropoja Basin. We rule out the former explanation because there is no evidence for a significant difference in the amount of precipitation in northern and southern Albania since the LGM (Wagner et al., 2019). The more likely explanation is therefore that the high incision rate in the Tropoja Basin marks the passage of the incision wave related to the first generation of knickpoints (yellow dots in **Figures 7, 10**) still found in the upper reaches of the Valbona River.

To summarize this chapter, the combination of ^{36}Cl ages of the fluvial terraces and geomorphic metric analysis show that river incision and sedimentation after the LGM was episodic. Prior to that, in the Early Pleistocene, a change from an internally to an externally drained system for the Drin River must have occurred as indicated by widespread lake sediments and relict topographic features mimicking former lake geometries. A tectonically controlled difference in base-level along the SPNF initially led to the formation of internally drained basins and lakes in the internal Dinarides which, like the Western Kosovo Basin and Tropoja Basin, lasted until Pliocene-to-Early Pleistocene time (Aliaj, 2006; Neubauer et al., 2015b; Pashko and Aliaj, 2020). Most of these basins no longer exist and evidence of their former presence is preserved as the flattened parts of river profiles draining from the hinterland to the Adriatic Sea (**Figure 8C**). Since Pliocene - Early Pleistocene time, drainage integration

involving over-spilling of lakes and, in the case of the Tropoja Basin, episodic breaching of dams would have resulted in regional drainage integration during the formation of the current Drin River. In the next section, we address the implications of potential drainage integration and shifts in drainage divides with respect to the Cenozoic faulting across Dinaric-Hellenic junction.

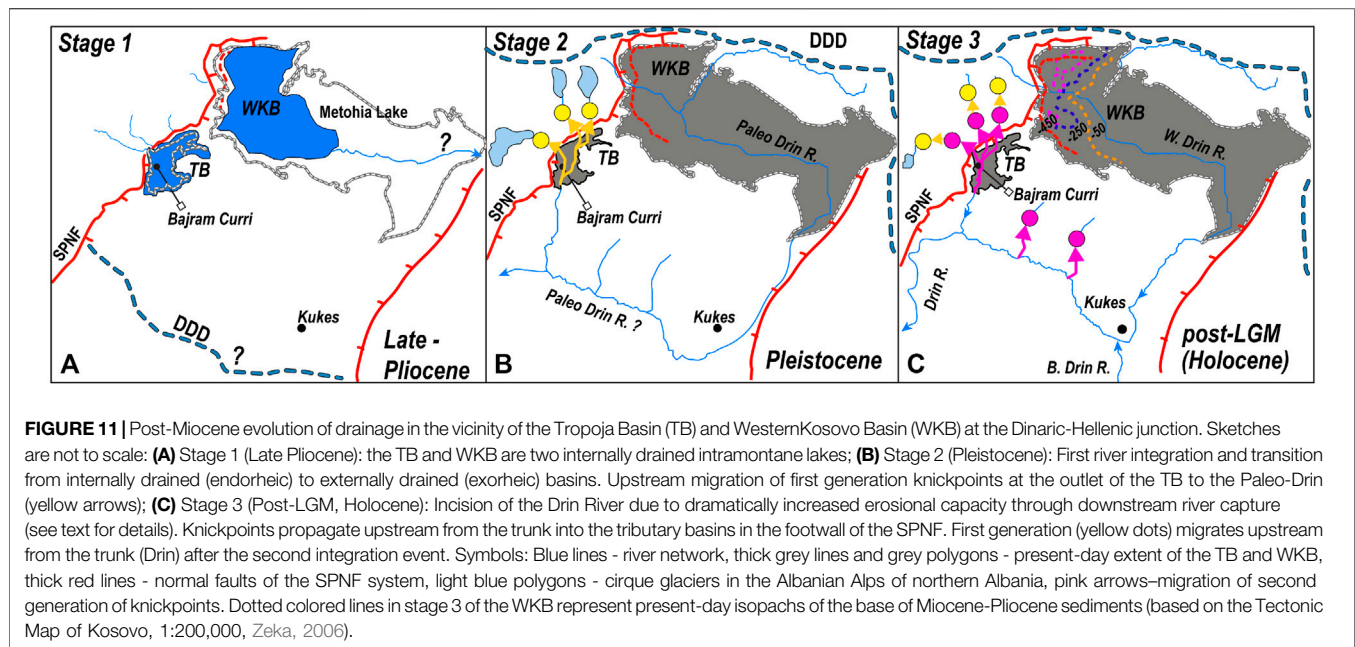
MODEL FOR POST-MIOCENE EVOLUTION OF LANDSCAPE AT THE DINARIC-HELLENIC JUNCTION

In the preceding chapters, we have documented how Cenozoic normal faults acted as a template upon which the last ice age substantially modified the landscape in this domain of tectonic bending at the Dinaric-Hellenic junction. Here, we present a conceptual model of how the post-Miocene rivers and lakes evolved in this structurally complex area (**Figure 11**). Three stages of landscape formation are discerned that account for the salient stratigraphic, palynological and fluvial features of the area (**Figure 11**).

During stage 1 (Late Pliocene, **Figure 11A**), two intramontane fresh-water lakes filled parts of the Western Kosovo Basin and Tropoja Basin (Meço and Aliaj, 2000; Aliaj et al., 2001; Neubauer, et al., 2015b; Pashko and Aliaj, 2020). By this stage, most if not all normal faulting along the SPNF had ceased, as indicated by basal Pliocene sediments that seal the subsurface branch of the SPNF beneath the Western Kosovo Basin (the Dukagjini Fault, Meço and Aliaj, 2000) and sub horizontal orientation of Plio-Pleistocene sediments in the Tropoja Basin (**Figure 4B**). The basins were internally drained (endorheic) at this stage, as supported by the evidence of quiet lacustrine sedimentation (marls in unit 1 of the Tropoja Basin, **Figures 4, 5**), the lack of any traces of fluvial down cutting and the absence of fluvial deposits downstream of the basins that, if present, would indicate basin drainage. The main drainage divide during stage 1 is therefore inferred to have been located to the WSW of the Western Kosovo Basin and Tropoja Basin, as drawn in **Figure 11A**. The base level for this paleo-drainage system is assumed to have been towards the SE, possibly into the Aegean Sea, but evidence is scarce.

We estimate an approximate accumulation rate of 0.1–0.2 mm/yr for stage 1 based on the 200–300 m thickness of Pliocene Late-Pleistocene lacustrine sediments in the southwestern part of the Western Kosovo Basin (Elazaj, 2012). These sedimentation rates are comparable with mean sedimentation rates in Lake Ohrid (**Figure 1**) of ~0.3–0.5 mm/yr since the Early-Pleistocene (Lindhorst et al., 2014). Based on this first-order estimate, the basin subsidence during stage 1 would have been higher than the sedimentation rate in the basin as evidenced by the deposition of lake sediments of the basal part of unit 1 and by evidence in Lake Ohrid for underfilled conditions since the Pliocene (Vogel et al., 2010b; Lindhorst et al., 2014).

Stage 2 (Pleistocene) was presaged in the Tropoja Basin by the deposition of sandstone in Unit 1 and the unconformable deposition of grey conglomerates of unit 2 (**Figure 4B**). This



unconformity at the base of unit 2 documents erosion under fluvial conditions in the Tropoja Basin that ushered in stage 2 (**Figure 11B**). We attribute this marked change from lacustrine to highly erosive fluvial conditions to basin drainage and river integration downstream of the basins. Similar transitions have been found to develop in fault-bounded extensional basins where fluvial sediments make up the uppermost part of the stratigraphy (e.g., Central Italian Apennines: Geurts et al., 2018; Geurts et al., 2020 and references therein). River integration occurs when basins and lakes overflow, spilling their water and inducing top-down erosion in intra-montane basins in the internal parts of orogens (Geurts et al., 2018). In the Tropoja Basin, overspilling of the Late Pliocene lake towards the end of stage 1 (**Figure 11A**) may have been augmented by melting of niche glaciers (Hughes, 2009) in the upper Valbona Valley, resulting in an increase of sediment and water supply.

The main drainage divide is depicted in **Figure 11** to have migrated upstream toward the internal part of the orogen between stages 1 and 2, thus reflecting the motion of headward erosion in response to river integration and capture of former lake areas. Stage 3 (Post LGM–Holocene?) was characterized by at least three pulses of river incision with related knickpoint migration (**Figure 11C**) and further drainage integration/capture within the regional river network. This stage corresponds to episodic fluvial downcutting and terracing in the Tropoja Basin. Overall, the changes in the rate of base-level rise from the LGM to the present controlled knickpoint formation and propagation upstream. This was modulated by late and/or post-LGM climatic fluctuations, as described in chapter 4. The coincidence of the two fluvial terraces in the Tropoja Basin dated at ~ 12 and ~8 ka with the two knickpoints in the tributary valleys of this basin (**Figure 9A**) suggests that two knickpoint generations migrated upstream following significant base-level changes during stage 3

(**Figure 11**). We infer that by stage 2, most of the basins were already externally drained (exorheic). This includes some, if not all, of the paleo-lakes whose former existence in the internal Dinarides is recorded by the flat parts of river profiles (**Figure 8C**).

CONCLUSION

In this paper, we show that the landscape at the Dinaric-Hellenic junction has undergone dramatic changes long after the cessation of the main Neogene activity of the normal faults of the SPNF that transect the mountain range. In particular, the most recent ice age enhanced depositional and erosional events in its aftermath that used the Cenozoic normal faults as a template for a strong morphological imprint. The first-order modification of the landscape during Pleistocene to Holocene time is perhaps best exemplified by the arcuate shape of the present drainage divide around the SPNF at the junction of Dinaric and Hellenic segments of the mountain belt. This fault and its related extensional structures helped localise Pleistocene to Holocene precipitation, erosion and deposition. The reorganization of fluvial drainage patterns leading to the formation and partial demise of lakes and basins.

Regarded at the scale of individual basins, the landscape reflects a subtle feedback between tectonic and climate-induced processes. Differential erosion fostered by the fault-induced juxtaposition of lithologies with contrasting erodibilities and possibly triggered by seismicity set the stage. But it was climatic variation, especially glaciation and subsequent melting, that increased erosion rates and changed the erosional base-level, facilitating a switch from internal to external drainage of lakes and basins into the Drin River. Our data show that river integration increased after the Last Glacial Maximum (LGM) when the Drin River drainage expanded its

upstream drainage area, leading to a top-down incision of the river system.

Overall, our data support the idea that rollback subduction in the Hellenides and associated extension, both parallel- and normal to the orogen, affected landscape formation. This happened because crustal extension accommodating slab steepening and bending localized faulting and induced basin subsidence. Normal faults like the SPNF control erodibility and provide river paths that focus erosion and sediment transport (e.g., Copley et al., 2009). Pliocene E-W orogen-normal extension is reflected by the present-day trace of the Black Drin, which runs parallel to the strike of the Dinaric thrusts, before cutting down to the Adriatic Sea parallel to the SPNF. Thus, slab dynamics in conjunction with post-LGM erosion at the Dinaric-Hellenic junction have exerted a first-order control on the geometry of the drainage patterns.

DATA AVAILABILITY STATEMENT

The original contributions presented in the study are included in the article/**Supplementary Material**, further inquiries can be directed to the corresponding author.

AUTHOR CONTRIBUTIONS

LG lead the study and wrote the manuscript, which was supplemented by substantial written contributions from MH, AR and JG, in consultation with KH, BM, MG and AB. Basic project funding was acquired by JG and MH with additional funding for cosmogenic dating obtained by LG and KH. BM, DS and MG conducted fieldwork and data analysis in the TB Basin supervised by LG, JG, MH and MG. BM performed the ³⁶Cl nuclides analysis and incision rates modelling supervised by LG and KH. LG and BM analysed the geomorphology and

interpreted it with input from AR and MH. AB aided in the sedimentological analysis of the basins.

FUNDING

Funding for our research came from the German Science Foundation in the form of Grants Gi 825/4-1 and Ha 2403/21-1, respectively, to co-authors JG and MH. This grant also supported the work of the first author, as well as the MSc work of co-authors DS and BM, and the PhD of MG. The TCN ages were made possible by a grant from RADIATE (Grant Agreement No. 19001937) to LG.

ACKNOWLEDGMENTS

We thank Naki Akçar (Univ. Bern), Jan Pleuger (FU-Berlin), Eline Le Breton (FU-Berlin), Dirk Scherler (GFZ/FU-Berlin) and Kujtim Onuzi (Univ. Tirana) for engaging discussions during the course of our work. Lab work was assisted by Philipp Hoelzmann and Frank Kutz (both FU-Berlin, major element compositions), Jessica A. Stammeier (ICP-MS trace element composition analysis), C. Vockenhuber (³⁶Cl research, support of MSc students at the Ion Beam Physics, Physics-LIP, Zurich), Olivia Steinemann-Kronig (support with terrestrial cosmogenic nuclides lab work), we acknowledge the remarks of the associated editor Gang Rao and reviewers Xianyan Wang and Huiping Zhang.

SUPPLEMENTARY MATERIAL

The Supplementary Material for this article can be found online at: <https://www.frontiersin.org/articles/10.3389/feart.2022.821707/full#supplementary-material>

REFERENCES

- Aliaj, S., Baldassarre, G., and Shkupi, D. (2001). Quaternary Subsidence Zones in Albania: Some Case Studies. *Bull. Eng. Geology. Environ.* 59, 313–318. doi:10.1007/s100640000063
- Aliaj, S. (2006). “The Albanian Orogen: Convergence Zone between Eurasia and the Adria Microplate,” in *The Adria Microplate: GPS Geodesy, Tectonics and Hazards. NATO Science Series IV: Earth and Environmental Sciences*. Editors N. Pinter, G. Grenerczy, J. Weber, S. Stein, and D. Medak (Springer), 133–149.
- Alley, R., and Ágústsdóttir, A. (2005). The 8k Event: Cause and Consequences of a Major Holocene Abrupt Climate Change. *Quat. Sci. Rev.* 24, 1123–1149. doi:10.1016/j.quascirev.2004.12.004
- Attal, M., Tucker, G. E., Whittaker, A. C., Cowie, P. A., and Roberts, G. P. (2008). Modeling Fluvial Incision and Transient Landscape Evolution: Influence of Dynamic Channel Adjustment. *J. Geophys. Res.* 113, F03013. doi:10.1029/2007JF000893
- Berlin, M. M., and Anderson, R. S. (2007). Modeling of Knickpoint Retreat on the Roan Plateau, Western Colorado. *J. Geophys. Res. Earth Surf.* 112 (F3). doi:10.1029/2006j000553
- Bordon, A., Peyron, O., Lézine, A.-M., Brewer, S., and Fouache, E. (2009). Pollen-inferred Late-Glacial and Holocene Climate in Southern Balkans (Lake Maliq). *Quat. Int.* 200 (Issues 1–2), 19–30. doi:10.1016/j.quaint.2008.05.014
- Braun, J., Gemignani, L., and van der Beek, P. (2018). Extracting Information on the Spatial Variability in Erosion Rate Stored in Detrital Cooling Age Distributions in River Sands. *Earth Surf. Dynam.* 6 (1), 257–270. doi:10.5194/esurf-6-257-2018
- Burchfiel, B. C., Nakov, R., Dumurdzanov, N., Papanikolaou, D., Tzankov, T., Serafimovski, T., et al. (2008). Evolution and Dynamics of the Cenozoic Tectonics of the South Balkan Extensional System. *Geosphere* 4 (6), 919–938. doi:10.1130/ges00169.1
- Caporali, A., Floris, M., Xue, C., Nurce, B., Bertocco, M., and Zurutuza, J. (2020). The November 2019 Seismic Sequence in Albania: Geodetic Constraints and Fault Interaction. *Remote Sensing* 12, 846. doi:10.3390/rs12050846
- Carcaillet, J., Mugnier, J. L., Koçi, R., and Jouanne, F. (2009). Uplift and Active Tectonics of Southern Albania Inferred from Incision of Alluvial Terraces. *Quat. Res.* 71, 465–476. doi:10.1016/j.yqres.2009.01.002
- Cavazza, W., Roure, F., and Ziegler, P. A. (2004). *The Mediterranean Area and the Surrounding regions: Active Processes, Remnant of Former Tethyan Oceans and Related Thrust Belts in: The TRANSMED Atlas: The Mediterranean Region from Crust to Mantle*. Springer Verlag Berlin Heidelberg. Available at: <https://www.springer.com/gp/book/9783540221814>.
- Christl, M., Vockenhuber, C., Kubik, P. W., Wacker, L., Lachner, J., Alfmov, V., et al. (2013). The ETH Zurich AMS Facilities: Performance Parameters and Reference Materials. *Nucl. Instr. Methods Phys. Res. Section B: Beam Interactions Mater. Atoms* 294, 29–38. doi:10.1016/j.nimb.2012.03.004

- Copley, A., Boait, F., Hollingsworth, J., Jackson, J., and McKenzie, D. (2009). Subparallel Thrust and normal Faulting in Albania and the Roles of Gravitational Potential Energy and Rheology Contrasts in Mountain Belts. *J. Geophys. Res.* 114, B05407. doi:10.1029/2008JB005931
- Crosby, B. T., and Whipple, K. X. (2006). Knickpoint Initiation and Distribution within Fluvial Networks: 236 Waterfalls in the Waipaoa River, North Island, New Zealand. *Geomorphology* 82 (1–2), 16–38. doi:10.1016/j.geomorph.2005.08.023
- D'Agostino, N., Jackson, J. A., Dramis, F., and Funicello, R. (2001). Interactions between Mantle Upwelling, Drainage Evolution and Active normal Faulting: an Example from the central Apennines (Italy). *Geophys. J. Internat.* 147, 475–497. doi:10.1046/j.1365-246x.2001.00539.x
- D'Agostino, N., Métois, M., Koci, R., Duni, L., Kuka, N., Ganas, A., et al. (2020). Active Crustal Deformation and Rotations in the Southwestern Balkans from Continuous GPS Measurements. *Earth Planet. Sci. Lett.* 539, 116246. doi:10.1016/j.epsl.2020.116246
- Dumurdjanov, N., Milutinovic, Z., and Salic, R. (2020). Seismotectonic Model Backing the PSHA and Seismic Zoning of Republic of Macedonia for National Annex to MKS EN 1998-1:2012 Eurocode 8. *J. Seismol* 24, 319–341. doi:10.1007/s10950-020-09912-9
- Dumurdzanov, N., Serafimovski, T., and Burchfiel, B. C. (2005). Cenozoic Tectonics of Macedonia and its Relation to the South Balkan Extensional Regime. *Geosphere* 1 (1), 1–22. doi:10.1130/ges00006.1
- Elezaj, Z., and Kodra, A. (2012). *Geology of Kosova (I)*. Pristina: Tekst Universitar.
- Flint, J. J. (1974). Stream Gradient as a Function of Order, Magnitude, and Discharge. *Water Resour. Res.* 10, 969–973. doi:10.1029/wr010i005p00969
- García-Castellanos, D. (2006). “Long-term Evolution of Tectonic Lakes: Climatic Controls on the Development of Internally Drained Basins,” in *Tectonics, Climate, and Landscape Evolution: Geological Society of America Special Paper 398, Penrose Conference Series*. Editors S. D. Willett, N. Hovius, M. T. Brandon, and D. M. Fisher, 283–294. doi:10.1130/2006.2398(17)
- García-Castellanos, D., and Villaseñor, A. (2011). Messinian Salinity Crisis Regulated by Competing Tectonics and Erosion at the Gibraltar Arc. *Nature* 480, 359–363. doi:10.1038/nature10651
- Gemignani, L., van der Beek, P. A., Braun, J., Najman, Y., Bernet, M., Garzanti, E., et al. (2018). Downstream Evolution of the Thermochronologic Age Signal in the Brahmaputra Catchment (Eastern Himalaya): Implications for the Detrital Record of Erosion. *Earth Planet. Sci. Lett.* 499, 48–61. doi:10.1016/j.epsl.2018.07.019
- Geurts, A. H., Cowie, P. A., Duclaux, G., Gawthorpe, R. L., Huisman, R. S., Pedersen, V. K., et al. (2018). Drainage Integration and Sediment Dispersal in active continental Rifts: a Numerical Modelling Study of the central Italian Apennines. *Basin Res.* 30 (5), 965–989. doi:10.1111/bre.12289
- Geurts, A. H., Whittaker, A. C., Gawthorpe, R. L., and Cowie, P. A. (2020). Transient Landscape and Stratigraphic Responses to Drainage Integration in the Actively Extending central Italian Apennines. *Geomorphology* 353, 107013. doi:10.1016/j.geomorph.2019.107013
- Gjani, E., and Dilek, Y. (2010). *Palynostratigraphy, Paleocology and Paleoclimatology of Tertiary Molasse Basins and the Peri-Adriatic Depression in albania and Paleogeographic Implications, Tectonic Crossroads: Evolving Orogens of Eurasia-Africa-Arabia*. Ankara, Turkey, 90. Available at: https://www.jmo.org.tr/resimler/ekler/6a6747117519d0d_ek.pdf.
- Gosse, J. C., and Phillips, F. M. (2001). Terrestrial *In Situ* Cosmogenic Nuclides: Theory and Application. *Quat. Sci. Rev.* 20, 1475–1560. doi:10.1016/s0277-3791(00)00171-2
- Hall, R., and Spakman, W. (2015). Mantle Structure and Tectonic History of SE Asia. *Tectonophysics* 658, 14–45. ISSN 0040-1951. doi:10.1016/j.tecto.2015.07.003
- Handy, M. R., Giese, J., Schmid, S. M., Pleuger, J., Spakman, W., Onuzi, K., et al. (2019). Coupled Crust-Mantle Response to Slab Tearing, Bending, and Rollback along the Dinaride-Hellenide Orogen. *Tectonics* 38, 2803–2828. doi:10.1029/2019tc005524
- Harkins, N., Kirby, E., Heimsath, A., Robinson, R., and Reiser, U. (2007). Transient Fluvial Incision in the Headwaters of the Yellow River, Northeastern Tibet, China. *J. Geophys. Res.* 112, F03S04. doi:10.1029/2006JF000570
- Herman, F., Seward, D., and Valla, P. (2013). Worldwide Acceleration of Mountain Erosion Under a Cooling Climate. *Nature* 504, 423–426. doi:10.1038/nature12877
- Hidy, A. J., Gosse, J. C., Pederson, J. L., Mattern, J. P., and Finkel, R. C. (2010). A Geologically Constrained Monte Carlo Approach to Modeling Exposure Ages from Profiles of Cosmogenic Nuclides: An Example from Lees Ferry, Arizona. *Geochem. Geophys. Geosystems* 11. doi:10.1029/2010gc003084
- Hughes, P. D. (2007). Recent Behaviour of the Debeli Namet Glacier, Durmitor, Montenegro. *Earth Surf. Process. Landforms* 32, 1593–1602. doi:10.1002/esp.1537
- Hughes, P. D. (2009). Twenty-first century Glaciers in the Prokletije Mountains, Albania. *Arctic, Antarctic Alpine Res.* 41, 455e459. doi:10.1657/1938-4246-41.4.455
- Ivy-Ochs, S., Poschinger, A. v., Synal, H.-A., and Maisch, M. (2009). Surface Exposure Dating of the Flims Landslide, Graubünden, Switzerland. *Geomorphology* 103, 104–112. doi:10.1016/j.geomorph.2007.10.024
- Ivy-Ochs, S., Synal, H.-A., Roth, C., and Schaller, M. (2004). Initial Results from Isotope Dilution for Cl and ³⁶Cl Measurements at the PSI/ETH Zurich AMS Facility. *Nucl. Instr. Methods Phys. Res. Section B: Beam Interactions Mater. Atoms* 223-224, 623–627. doi:10.1016/j.nimb.2004.04.115
- Jaupaj, O., Lamaj, M., Kulici, H., Jusufati, M., Plaku, E., and Gjeta, I. (2017). “Landslide Inventory Map of Albania,” in *Advancing Culture of Living with Landslides. WLF 2017*. Editors M. Mikos, B. Tiwari, Y. Yin, and K. Sassa (Cham: Springer). doi:10.1007/978-3-319-53498-5_5
- Jolivet, L., and Brun, J.-P. (2010). Cenozoic Geodynamic Evolution of the Aegean. *Int. J. Earth Sci. (Geol Rundsch)* 99, 109–138. doi:10.1007/s00531-008-0366-4
- Jouanne, F., Mugnier, J. L., Koci, R., Bushati, S., Matev, K., Kuka, N., et al. (2012). GPS Constraints on Current Tectonics of Albania. *Tectonophysics* 554-557, 50–62. doi:10.1016/j.tecto.2012.06.008
- Kirby, E., and Whipple, K. (2001). Quantifying Differential Rock-Uplift Rates via Stream Profile Analysis. *Geol* 29, 415–418. doi:10.1130/0091-7613(2001)029<0415:qdrurv>2.0.co;2
- Kirby, E., and Whipple, K. X. (2012). Expression of Active Tectonics in Erosional Landscapes. *J. Struct. Geology*. 44, 54–75. doi:10.1016/j.jsg.2012.07.009
- Kissel, C., Speranza, F., and Milicevic, V. (1995). Paleomagnetism of External Southern and central Dinarides and Northern Albanides: Implications for the Cenozoic Activity of the Scutari-Pec Transverse Zone. *J. Geophys. Res.* 100 (B8), 14999–15007. doi:10.1029/95jb01243
- Kuhlemann, J., Milivojević, M., Krumrei, I., and Kubik, P. W. (2009). Last Glaciation of the Sara Range (Balkan peninsula): Increasing Dryness from the LGM to the Holocene. *Austrian J. Earth Sci.* 102, 146e158.
- Lacey, J. H., Leng, M. J., Francke, A., Sloane, H. J., Milodowski, A., Vogel, H., et al. (2016). Northern Mediterranean Climate since the Middle Pleistocene: a 637 Ka Stable Isotope Record from Lake Ohrid (Albania/Macedonia). *Biogeosciences* 13, 1801–1820. doi:10.5194/bg-13-1801-2016
- Lambeck, K., and Bard, E. (2000). Sea-level Change along the French Mediterranean Coast for the Past 30 000 Years. *Earth Planet. Sci. Lett.* 175, 203–222. doi:10.1016/s0012-821x(99)00289-7
- Lambeck, K., and Purcell, A. (2005). Sea-level Change in the Mediterranean Sea since the LGM: Model Predictions for Tectonically Stable Areas. *Quat. Sci. Rev.* 24 (Issues 18–19), 1969–1988. doi:10.1016/j.quascirev.2004.06.025
- Lavé, J., and Avouac, J. P. (2001). Fluvial Incision and Tectonic Uplift across the Himalayas of central Nepal. *J. Geoph. Res.* 106, 561–591. doi:10.1029/2001jb000359
- Lindhorst, K., Krastel, S., Reicherter, K., Stipp, M., Wagner, B., and Schwenk, T. (2014). Sedimentary and Tectonic Evolution of Lake Ohrid (Macedonia/Albania). *Basin Res.* 27 (1), 84–101. doi:10.1111/bre.12063
- Macklin, M. G., Fuller, I. C., Lewin, J., Maas, G. S., Passmore, D. G., Rose, J., et al. (2002). Correlation of Fluvial Sequences in the Mediterranean basin over the Last 200ka and Their Relationship to Climate Change. *Quat. Sci. Rev.* 21, 1633–1641. doi:10.1016/s0277-3791(01)00147-0
- Mair, D., Lechmann, A., Yesilyurt, S., Tikhomirov, D., Delunel, R., Vockenhuber, C., et al. (2019). Fast Long-Term Denudation Rate of Steep alpine Headwalls Inferred from Cosmogenic ³⁶Cl Depth Profiles. *Sci. Rep.* 9, 11023. doi:10.1038/s41598-019-46969-0
- Malatesta, L. C., Prancevic, J. P., and Avouac, J. P. (2017). Autogenic Entrenchment Patterns and Terraces Due to Coupling with Lateral Erosion in Incising Alluvial Channels. *J. Geophys. Res. Earth Surf.* 122, 335–355. doi:10.1002/2015JF003797
- Marc, O., Hovius, N., Meunier, P., Uchida, T., and Hayashi, S. (2015). Transient Changes of Landslide Rates after Earthquakes. *Geology* 43 (10), 883–886. doi:10.1130/g36961.1
- Marrucci, M., Zeilinger, G., Ribolini, A., and Schwanghart, W. (2018). Origin of Knickpoints in an Alpine Context Subject to Different Perturbing Factors, Stura Valley, Maritime Alps (North-Western Italy). *Geosciences* 8 (12). doi:10.3390/geosciences8120443

- Matenco, L., and Radivojević, D. (2012). On the Formation and Evolution of the Pannonian Basin: Constraints Derived from the Structure of the Junction Area between the Carpathians and Dinarides. *Tectonics* 31, a–n. Article TC6007. doi:10.1029/2012TC003206
- Meço, S., and Aliaj, S. (2000). *Geology of Albania*. Berlin, Stuttgart: Gebrüder Borntraeger, 246.
- Milivojević, M., Menković, L., and Čalić, J. (2008). Pleistocene Glacial Relief of the central Part of Mt. Prokletije (Albanian Alps). *Quat. Int.* 190, 112–122.
- Muceku, B., van der Beek, P., Bernet, M., Reiners, P., Mascle, G., and Tashko, A. (2008). Thermochronological Evidence for Mio-Pliocene Late Orogenic Extension in the north-eastern Albanides (Albania). *Terra Nova* 20 (3), 180–187. doi:10.1111/j.1365-3121.2008.00803.x
- Muhs, D. R., Budahn, J., Avila, A., Skipp, G., Freeman, J., and Patterson, D. (2010). The Role of African Dust in the Formation of Quaternary Soils on Mallorca, Spain and Implications for the Genesis of Red Mediterranean Soils. *Quat. Sci. Rev.* 29, 2518–2543. doi:10.1016/j.quascirev.2010.04.013
- Muço, B., Alexiev, G., Aliaj, S., Elezi, Z., Grecu, B., Mandrescu, N., et al. (2012). Geohazards Assessment and Mapping of Some Balkan Countries. *Nat. Hazards* 64, 943–981. doi:10.1007/s11069-012-0185-6
- Muço, B. (1995). The Seasonality of Albanian Earthquakes and Cross-Correlation with Rainfall. *Phys. Earth Planet. Interiors* 88 (Issues 3–4), 285–291. doi:10.1016/0031-9201(94)02988-n
- NASA (2013). Shuttle Radar Topography Mission (SRTM) Global. *Distributed by OpenTopography*. doi:10.5069/G9445JDFAccessed 03 02, 2021
- Neely, A. B., Bookhagen, B., and Burbank, D. W. (2017). An Automated Knickzone Selection Algorithm (KZ-Picker) to Analyze Transient Landscapes: Calibration and Validation. *J. Geophys. Res. Earth Surf.* 122, 1236–1261. doi:10.1002/2017JF004250
- Neubauer, T. A., Harzhauser, M., Georgopoulou, E., Mandic, O., and Mandic, A. (2015b). Tectonics, Climate, and the Rise and Demise of continental Aquatic Species Richness Hotspots. *Proc. Natl. Acad. Sci. U S A* 112, 11478–11483. doi:10.1073/pnas.1503992112
- Ott, F., Gallen, S. F., Caves Rugenstein, J. K., Ivy-Ochs, S., Helman, D., Charalamos, F., et al. (2019). *Chemical versus Mechanical Denudation in Meta-Clastic and Carbonate Bedrock Catchments on Crete, Greece, and Mechanisms for Steep and High Carbonate Topography*. Available at: <https://agupubs.onlinelibrary.wiley.com/doi/10.1029/2019JF005142#>.
- Pashko, P., and Aliaj, S. (2020). Stratigraphy and Tectonic Evolution of Late Miocene - Quaternary Basins in Eastern Albania: A Review. *geosociety* 56, 317–351. doi:10.12681/bgsg.22064
- Pazzaglia, F. (2013). *River Terraces. Treatise of Geomorphology*. New York: Elsevier, 379412.
- Perron, J. T., and Royden, L. (2013). An Integral Approach to Bedrock River Profile Analysis. *Earth Surf. Process. Landforms* 38, 570–576. doi:10.1002/esp.3302
- Pirazzoli, P. A. (1991). *World Atlas of Holocene Sea-Level Changes*, 58. Amsterdam, London, New York, Tokyo: Elsevier Oceanography Series.
- Piomallo, C., and Morelli, A. (2003). P Wave Tomography of the Mantle Under the Alpine-Mediterranean Area. *J. Geophys. Res.* 108, 2065. doi:10.1029/2002JB001757
- Royden, L. (1996). Coupling and Decoupling of Crust and Mantle in Convergent Orogens: Implications for Strain Partitioning in the Crust. *J. Geophys. Res.* 101, 17679–17705. doi:10.1029/96JB00951
- Royden, L., and Taylor Perron, J. (2013). Solutions of the Stream Power Equation and Application to the Evolution of River Longitudinal Profiles. *J. Geophys. Res. Earth Surf.* 118, 497–518. doi:10.1002/jgrf.20031
- Schaller, M., Ehlers, T. A., Blum, J. D., and Kallenberg, M. A. (2009). Quantifying Glacial Moraine Age, Denudation, and Soil Mixing with Cosmogenic Nuclide Depth Profiles. *J. Geophys. Res. Earth Surf.* 114 (F1). doi:10.1029/2007Jf000921
- Schmid, S. M., Bernoulli, D., Fügenschuh, B., Matenco, L., Schefer, S., Schuster, R., et al. (2008). The Alpine-Carpathian-Dinaridic Orogenic System: Correlation and Evolution of Tectonic Units. *Swiss J. Geosci.* 101 (1), 139–183. doi:10.1007/s00015-008-1247-3
- Schwanghart, W., and Scherler, D. (2017). Bumps in River Profiles: Uncertainty Assessment and Smoothing Using Quantile Regression Techniques. *Earth Surf. Dynam.* 5, 821–839. doi:10.5194/esurf-5-821-2017
- Schwanghart, W., and Scherler, D. (2020). Divide Mobility Controls Knickpoint Migration on the Roan Plateau (Colorado, USA). *Geology* 48 (7), 698–702. doi:10.1130/g47054.1
- Schwanghart, W., and Scherler, D. (2014). Short Communication: TopoToolbox 2 - MATLAB-Based Software for Topographic Analysis and Modeling in Earth Surface Sciences. *Earth Surf. Dynam.* 2, 1–7. doi:10.5194/esurf-2-1-2014
- Snyder, N. P., Whipple, K. X., Tucker, G. E., and Merritts, D. J. (2000). Landscape Response to Tectonic Forcing: Digital Elevation Model Analysis of Stream Profiles in the Mendocino Triple Junction Region, Northern California. *GSA Bulletin* 112, 1250–1263. doi:10.1130/0016-7606(2000)112
- Speranza, F., Islami, I., Kissel, C., and Hyseni, A. (1995). Paleomagnetic Evidence for Cenozoic Clockwise Rotation of the External Albanides. *Earth Planet. Sci. Lett.* 129 (1–4), 121–134. doi:10.1016/0012-821x(94)00231-m
- Stock, J. D., and Dietrich, W. E. (2006). Erosion of Steepland Valleys by Debris Flows. *Geol. Soc. America Bull.* 118 (9–10), 1125–1148. doi:10.1130/B25902.1
- Stokes, M., Mather, A. E., and Harvey, A. M. (2002). Quantification of River-Capture-Induced Base-Level Changes and Landscape Development, Sorbas Basin, SE Spain. *Geol. Soc. Lond. Spec. Publications* 191, 23–35. doi:10.1144/gsl.sp.2002.191.01.03
- Tucker, G. E., McCoy, S. W., Whittaker, A. C., Roberts, G. P., Lancaster, S. T., and Phillips, R. (2011). Geomorphic Significance of Postglacial Bedrock Scarps on normal Fault Footwalls. *J. Geophys. Res. Earth Surf.* 116 (F1). doi:10.1029/2010Jf001861
- Tucker, G. E., and Slingerland, R. (1997). Drainage basin Responses to Climate Change. *Water Resour. Res.* 33 (8), 2031–2047. doi:10.1029/97wr00409
- Unen, M. V., Matenco, L., Nader, F. H., Darnault, R., Mandić, O., and Demir, V. (2018). Kinematics of Foreland-vergent Crustal Accretion: Inferences from the Dinarides Evolution. *Tectonics* 38, 49–76. doi:10.1029/2018TC005066
- Vogel, H., Wagner, B., Zanchetta, G., Sulpizio, R., and Rosén, P. (2010a). A Paleoclimate Record with Tephrochronological Age Control for the Last Glacial-Interglacial Cycle from Lake Ohrid, Albania and Macedonia. *J. Paleolimnol.* 44, 295–310. doi:10.1007/s10933-009-9404-x
- Vogel, H., Wessels, M., Albrecht, C., Stich, H.-B., and Wagner, B. (2010b). Spatial Variability of Recent Sedimentation in Lake Ohrid (Albania/Macedonia). *Biogeosciences* 7, 3333–3342. doi:10.5194/bg-7-3333-2010
- Wagner, B., Aufgebauer, A., Vogel, H., Zanchetta, G., Sulpizio, R., and Damaschke, M. (2012). Late Pleistocene and Holocene Contourite Drift in Lake Prespa (Albania/F.Y.R. Of Macedonia/Greece). *Quat. Int.* 274, 112–121. doi:10.1016/j.quaint.2012.02.016
- Wagner, B., Vogel, H., Francke, A., Friedrich, T., Donders, T., Lacey, J. H., et al. (2019). Mediterranean winter Rainfall in Phase with African Monsoons during the Past 1.36 Million Years. *Nature* 573, 256–260. doi:10.1038/s41586-019-1529-0
- Whipple, K. X., Forte, A. M., DiBiase, R. A., Gasparini, N. M., and Ouimet, W. B. (2017). Timescales of Landscape Response to divide Migration and Drainage Capture: Implications for the Role of divide Mobility in Landscape Evolution. *J. Geophys. Res. Earth Surf.* 122, 248–273. doi:10.1002/2016JF003973
- Whipple, K. X. (2009). The Influence of Climate on the Tectonic Evolution of Mountain Belts. *Nat. Geosci* 2, 97–104. doi:10.1038/ngeo413
- Whipple, K. X., and Tucker, G. E. (1999). Dynamics of the Stream-Power River Incision Model: Implications for Height Limits of Mountain Ranges, Landscape Response Timescales, and Research Needs. *J. Geophys. Res.* 104 (B8), 17661–17674. doi:10.1029/1999jb900120
- Whittaker, A. C., and Boulton, S. J. (2012). Tectonic and Climatic Controls on Knickpoint Retreat Rates and Landscape Response Times. *J. Geophys. Res. Earth Surf.* 117 (F2). doi:10.1029/2011Jf002157
- Whittaker, A. C., Cowie, P. A., Attal, M., Tucker, G. E., and Roberts, G. P. (2007). Bedrock Channel Adjustment to Tectonic Forcing: Implications for Predicting River Incision Rates. *Geology* 35 (2), 103–106. doi:10.1130/g23106a.1
- Whittaker, A. C. (2012). How Do Landscapes Record Tectonics and Climate? *Lithosphere* 4 (2), 160–164. doi:10.1130/rlf003.1
- Willett, S. D., McCoy, S. W., Perron, J. T., Goren, L., and Chen, C. Y. (2014). Dynamic Reorganization of River Basins. *Science* 343 (6175), 1248765. doi:10.1126/science.1248765
- Wobus, C., Whipple, K., Kirby, E., Snyder, N., Johnson, J., Spyropolou, K., et al. (2006). “Tectonics from Topography: Procedures, Promise and Pitfalls.”

- Tectonics, Climate and Landscape Evolution*. Editor S. D. Willett (Colorado, United States: Geol. Soc. Am), 398, 55–74. doi:10.1130/2006.2398(04)
- Wobus, C. W., Tucker, G. E., and Anderson, R. S. (2010). Does Climate Change Create Distinctive Patterns of Landscape Incision? *J. Geophys. Res.* 115, F04008. doi:10.1029/2009jf001562
- Wortel, M. J. R., and Spakman, W. (2000). Subduction and Slab Detachment in the Mediterranean-Carpathian Region. *Science* 290, 1910–1917. doi:10.1126/science.290.5498.1910
- Xhomo, A., Kodra, A., Xhafa, Z., and Shallo, M. (2002). *Geological Map of Albania, Scale 1: 200,000*. Tirana, Albania: AGS. Tirana 408.
- Yang, R., Willett, S. D., and Goren, L. (2015). *In Situ* low-relief Landscape Formation as a Result of River Network Disruption. *Nature* 520 (7548), 526–529. doi:10.1038/nature14354
- Zeka, N. (2006). *Tectonic Map of Kosovo, Scale 1: 200,000*. Independent Commission for Mines and Minerals Komisioni i Pavarur për Miniera dhe Minerale Nezavisna Komisija za Rudnike i Minerale Governing Board Rr. Rrustem Statovci 29 Prishtinë, Kosovo Chairman: Naip Zeka. Available at: www.kosovo-mining.org.

Conflict of Interest: The authors declare that the research was conducted in the absence of any commercial or financial relationships that could be construed as a potential conflict of interest.

Publisher's Note: All claims expressed in this article are solely those of the authors and do not necessarily represent those of their affiliated organizations, or those of the publisher, the editors and the reviewers. Any product that may be evaluated in this article, or claim that may be made by its manufacturer, is not guaranteed or endorsed by the publisher.

Copyright © 2022 Gemignani, Mittelbach, Simon, Rohrmann, Grund, Bernhardt, Hippe, Giese and Handy. This is an open-access article distributed under the terms of the Creative Commons Attribution License (CC BY). The use, distribution or reproduction in other forums is permitted, provided the original author(s) and the copyright owner(s) are credited and that the original publication in this journal is cited, in accordance with accepted academic practice. No use, distribution or reproduction is permitted which does not comply with these terms.